

Charm Production in CC DIS at HERA

Jae D. Nam

Temple Univ.

Motivations

- Charm cross section measurement in high- Q^2 charged current (CC) DIS.
→ Constraints on $s(x, Q^2)$
- Previous measurements on strangeness of the proton.
→ CCFR/NuTeV : $\frac{\int_0^1 dx[xs+x\bar{s}]}{\int_0^1 dx[x\bar{u}+x\bar{d}]}$ ~ 0.5 at $x \sim 0.1$, $Q^2 \sim 10 \text{ GeV}^2$
→ ATLAS : $\frac{s+\bar{s}}{\bar{u}+\bar{d}}$ ~ 1.0 at $x = 0.023, Q^2 = 1.9 \text{ GeV}^2$
- Improved determination of strange sea quark content in the proton (right)
 - Charm production in neutrino-nucleon scattering by CCFR/NuTeV, NOMAD, CHORUS
 - $W + c$ production by CMS and ATLAS

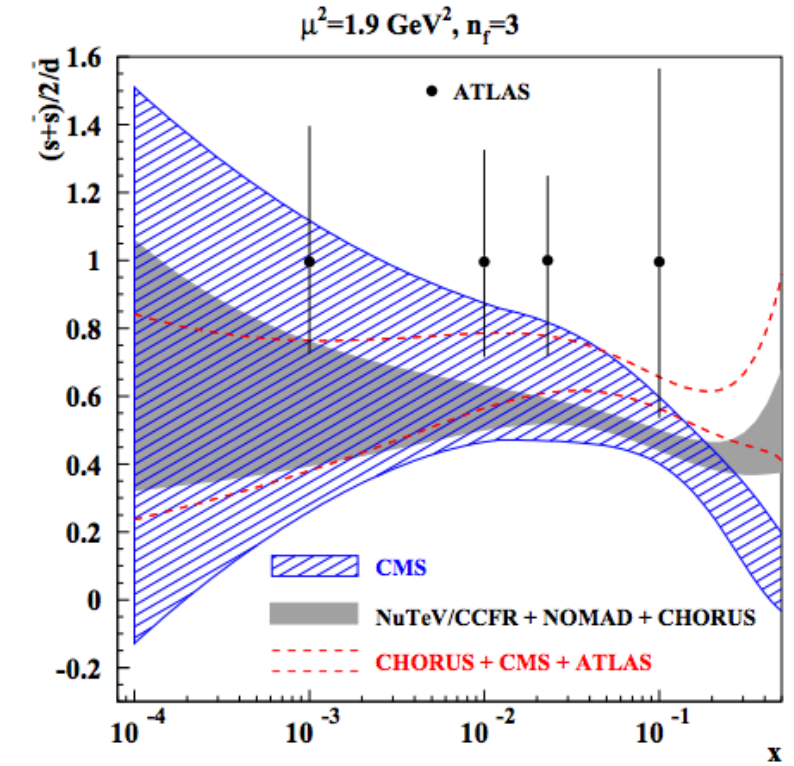
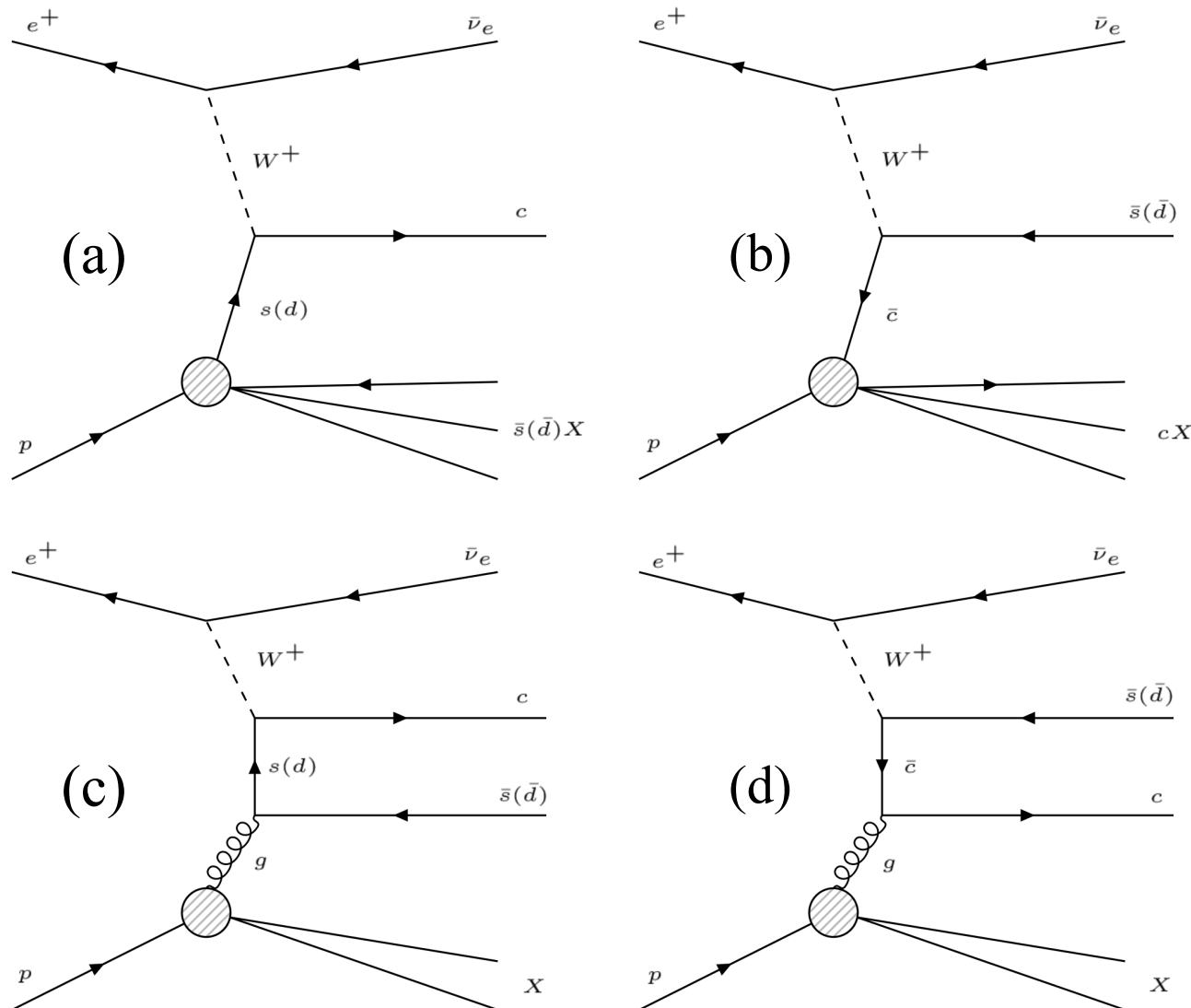
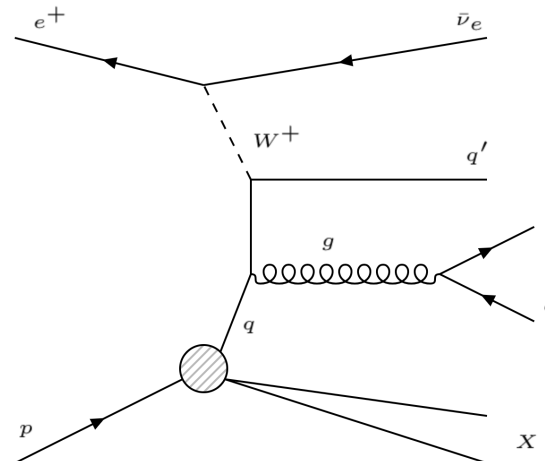


FIG. V.1: The 1σ band for the strange sea suppression factor $r_s = (s + \bar{s})/2\bar{d}$ as a function of the Bjorken x obtained in the variants of present analysis based on the combination of the data by NuTeV/CCFR [2], CHORUS [4], and NOMAD [3] (shaded area) and CHORUS [4], CMS [10], and ATLAS [11] (dashed lines), in comparison with the results obtained by the CMS analysis [10] (hatched area) and by the ATLAS $epWZ$ -fit [9, 11] at different values of x (full circles). All quantities refer to the factorization scale $\mu^2 = 1.9 \text{ GeV}^2$.

Charm production in CCDIS at HERA



- QPM-like processes (a, b)
 - Small active charm content in the proton.
→ small contribution of (b)
 - Cabibbo-suppressed $d \rightarrow c$ transition.
 - Sensitive to the strangeness in the proton.
- BGF-like processes (c, d)
 - Sensitive to the gluon content in the proton.
 - Model-dependent strange quark content extraction.
 - Final state gluon splitting (below).



DATA & MC & Kinematic variables

Data

- HERA II ($L \cong 360 \text{ pb}^{-1}$)
 - e^-p : 05e, 06e w/ $L \cong 185 \text{ pb}^{-1}$
 - e^+p : 0304p, 0607p w/ $L \cong 173 \text{ pb}^{-1}$

Year	Collision	Integrated Luminosity (pb^{-1})
2003/04	e^+p	~ 38
2004/05	e^-p	~ 133
2006	e^-p	~ 52
2006/07	e^+p	~ 135

MC

- DIS
 - Inclusive CCDIS MC, DJANGOH 1.6, ARIADNE 4.12, CTEQ-5D.
- Background
 - Inclusive NCDIS MC: DJANGOH 1.6, ARIADNE 4.12, CTEQ-5D
 - Photoproduction MC: HERWIG, resolved & direct
 - Background contribution was found to be negligible.

- Invariant kinematic variables (x, y, Q^2) defined by using Jacquet-Blondel Method.

$$y_{JB} = \frac{\sum_h (E - p_z)_h}{2E_{e,beam}}$$

$$Q_{JB}^2 = \frac{p_{T,h}^2}{1 - y_{JB}}$$

$$x_{JB} = \frac{Q_{JB}^2}{sy_{JB}}$$

DIS Selection Summary

General Selection	
Trigger	FLT 60 63 39 40 41 43 44 SLT EXO 4 TLT EXO 2 EXO 6 DST 34
DQ	EVTAKE, POLTAKE, MVDTAKE, STTTAKE
p_T	$p_T > 12 \text{ GeV}$ $p'_T > 10 \text{ GeV}$
Kinematic	$200 < Q^2 < 60,000 \text{ GeV}^2$ $y < 0.9$
Tracking Based Selection	
Vertex	$ Z_{\text{vtx}} < 30 \text{ cm}$
$\phi_{\text{cal}} - \phi_{\text{trk}}$	$d\phi < 90 \text{ degrees}$
Beam Gas	$N_{\text{trkvtx}} > 0.125 * (N_{\text{trk}} - 20)$
Trk	

**Based on 0607p CC MC by Ciesielski & Oliver

Calorimeter Based Selection	
Timing	Consistent with ep interaction
PhP, Beam Gas	$V_{\text{ap}}/V_p < 0.25$ if ($P_T < 20 \text{ GeV}$) $V_{\text{ap}}/V_p < 0.35$ else
Cosmics	Reject if: $N_{\text{cell}} < 40$ or (BAC/BRMU cosmic muon) or $E_{\text{RCAL}} > 2 \text{ GeV}$ and $f_{\text{RHAC}} > 0.5$ or $E_{\text{BCAL}} > 2 \text{ GeV}$ and $f_{\text{BHAC}} > 0.85$ or $f_{\text{BHAC1}} > 0.7$ or $f_{\text{BHAC2}} > 0.4$ or $E_{\text{FCAL}} > 2 \text{ GeV}$ and $f_{\text{FHAC}} < 0.10$ or $f_{\text{FHAC}} > 0.85$ or $f_{\text{FHAC1}} > 0.7$ or $f_{\text{FHAC2}} > -.6$
Halo Muon	Reject if: $\text{MaxEtCell_nr} \leq 16384$ and $\text{RCAL asosE} > 0.3 \text{ GeV}$ (FCAL) or $T_{\text{sub}}_{\text{halo}} > 0$ (TSUBAME in BCAL) or (BAC/BRMU halo muon)
NC DIS	Reject if: $PT < 30 \text{ GeV} \&\& E_{\text{-Pz}} > 30 \text{ GeV} \&\& E_{\text{-e}} > 4 \text{ GeV} \&\& E_{\text{-in}} < 5 \text{ GeV}$ $\&\& (P_{\text{trk}}/E_{\text{e}} > 0.25 \text{ for } 15 < \theta_{\text{e}} < 164 \text{ or } E_{\text{te}} > 2 \text{ GeV for } \theta_{\text{e}} > 164)$

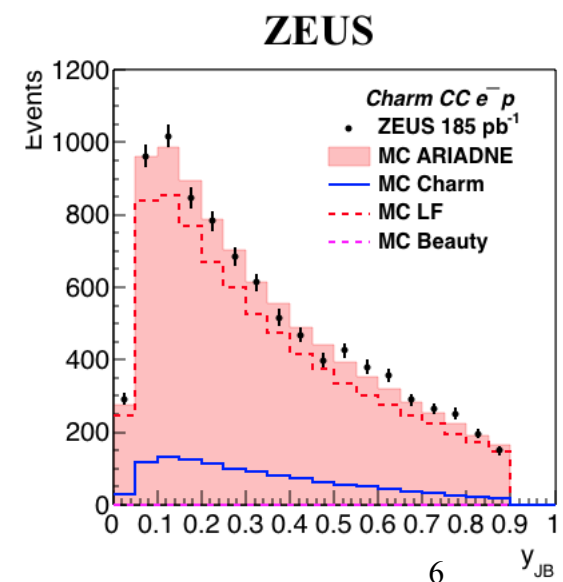
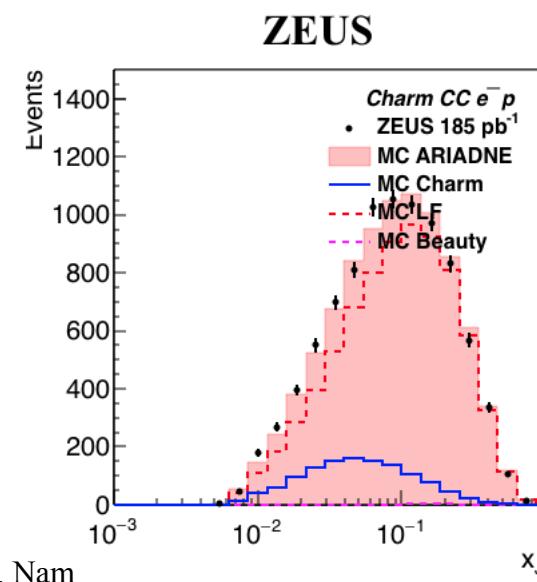
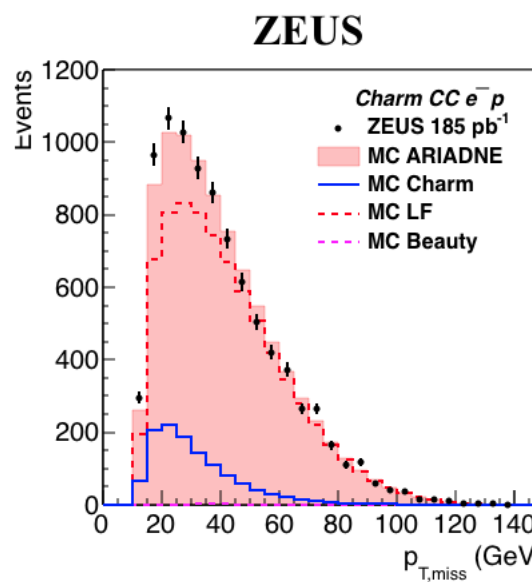
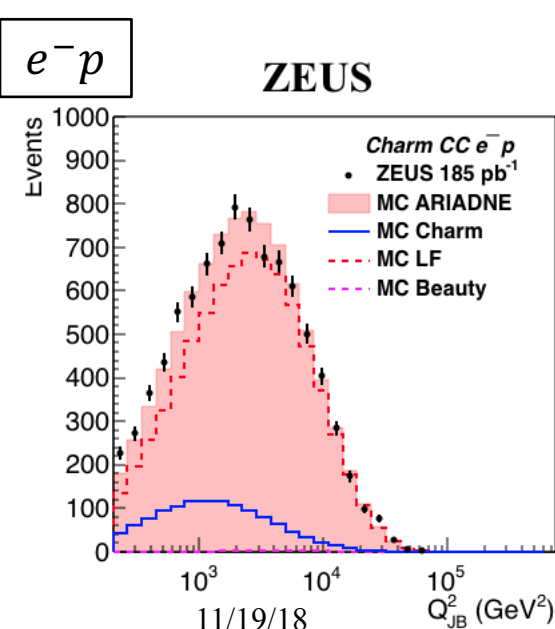
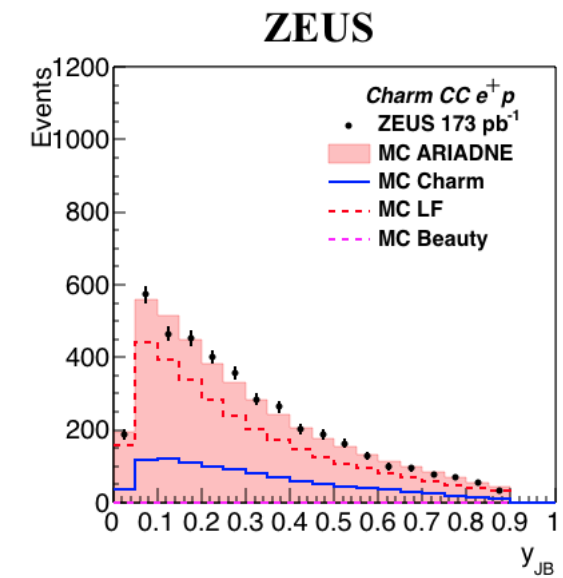
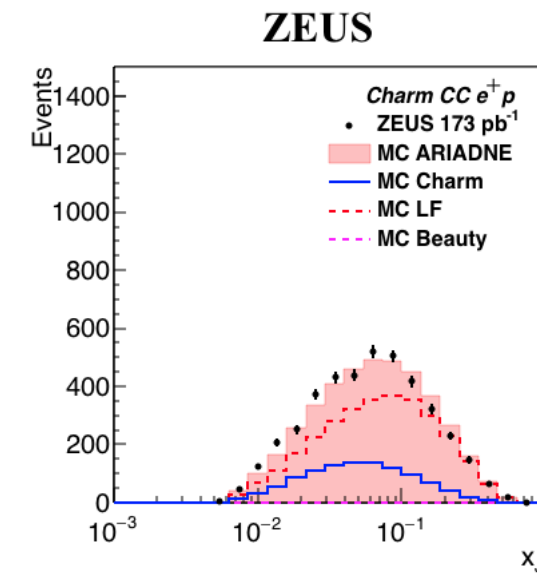
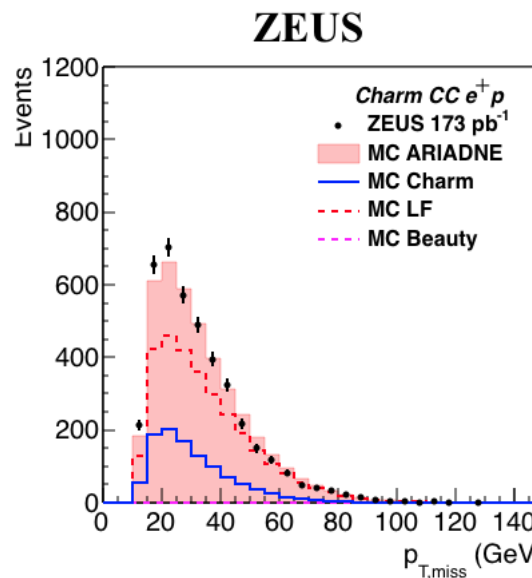
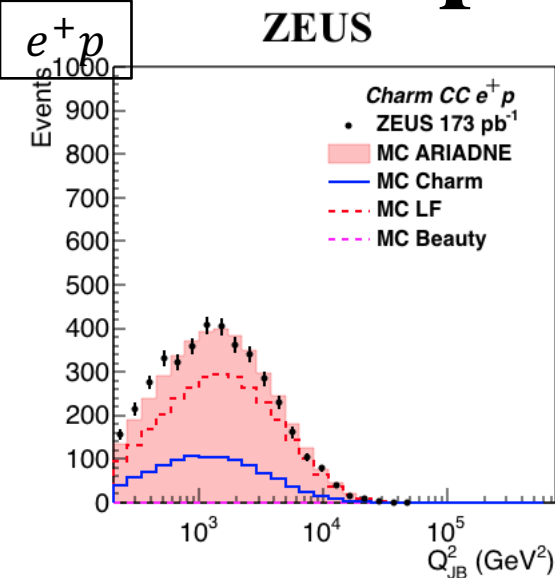
yellow – Varies between run periods

-STTTAKE = 0 for 05e data
-FLT 63 active after run 54115

green – Only applied on data

-Timing cut only on data

Control plots – event



Jae D. Nam

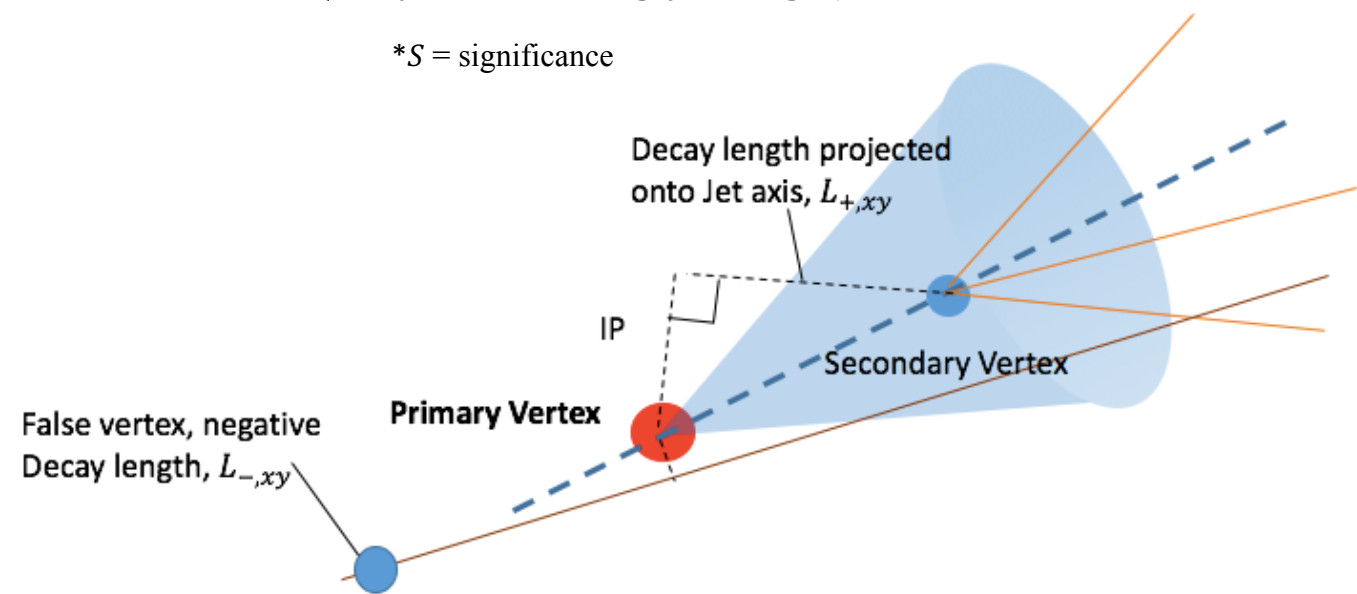
Charm Identification

Lifetime-tagging Method

- 2D decay length (L_{xy}) projected onto Jet axis.
 - LF \rightarrow Short-lived, Symmetric decay length.
 - Charm \rightarrow Long-lived, Asymmetric.
- LF contribution (background) suppressed by mirroring decay length distribution about $L_{xy} = 0$.

$$(N_{L+} - N_{L-}, N_{S+} - N_{S-})$$

* S = significance



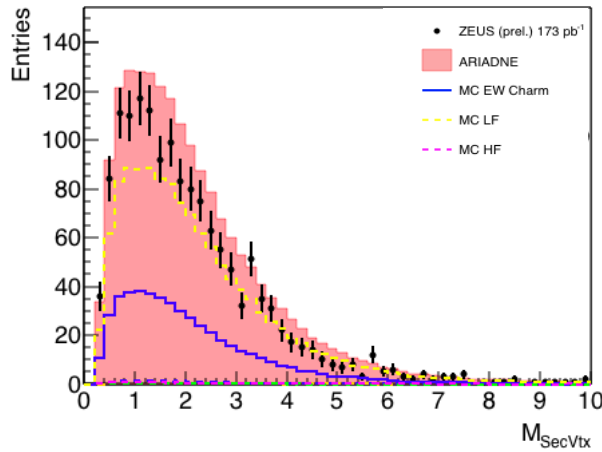
Jet Selection	Reconstructed by using kT algorithm in the massive mode.
	$E_T^{jet} > 5 \text{ GeV}$
	$-2.5 < \eta^{jet} < 2.0$ (1.5 for $05e$)
SecVtx Selection	$\chi^2/N_{dof} < 6$
	$ Z_{secvtx} < 30 \text{ cm}$
	Distance to beam spot $\sqrt{\Delta x^2 + \Delta y^2} < 1 \text{ cm}$
	$M_{secvtx} < 6 \text{ GeV}$
	$N_{secvtx}^{trk} > 2$

- E_T^{jet} and η^{jet} cuts further define the kinematic phase space of the measurement.

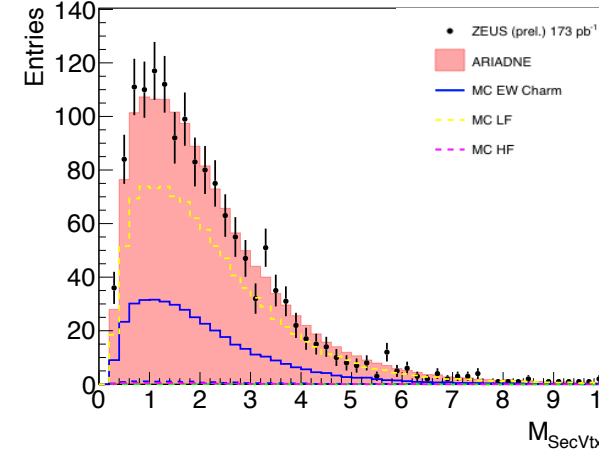
Secondary Vertex Scaling

(0607p)

Secondary Vertex Mass

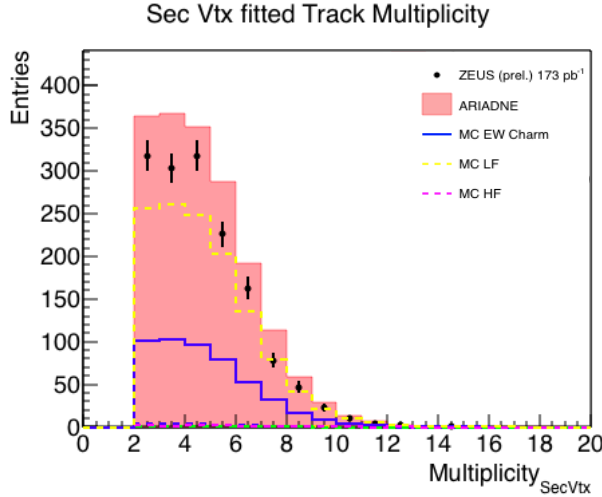


Secondary Vertex Mass

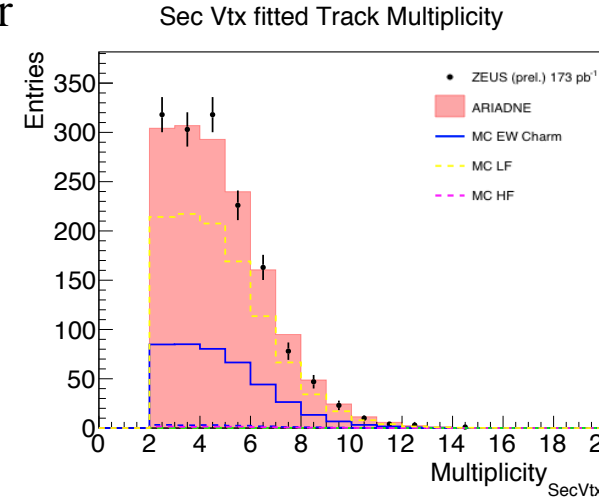


- MC overestimates trackings & secondary vertices.
- A secondary scaling applied to MC to match Data.

$$\begin{aligned} N_{SecVtx}^{DATA}/N_{SecVtx}^{MC} &= 0.708 \text{ (0304p)} \\ &= 0.810 \text{ (05e)} \\ &= 0.807 \text{ (06e)} \\ &= 0.830 \text{ (0607p)} \end{aligned}$$



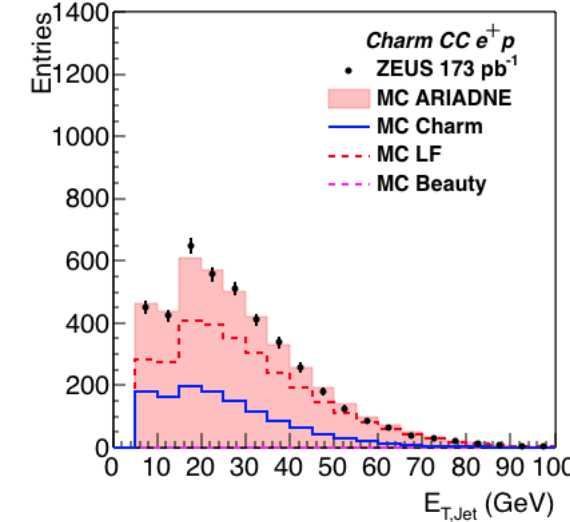
MC scaling factor
= 0.830



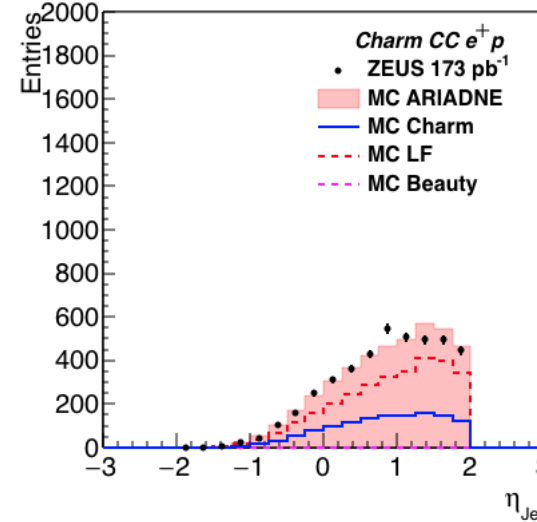
Control plots – jet & secondary vertex

$e^+ p$

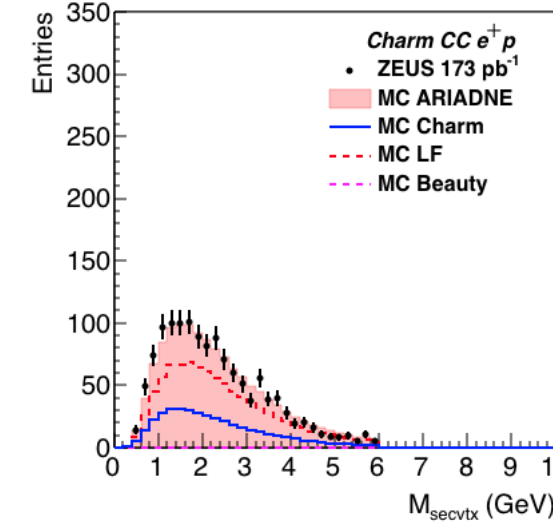
ZEUS



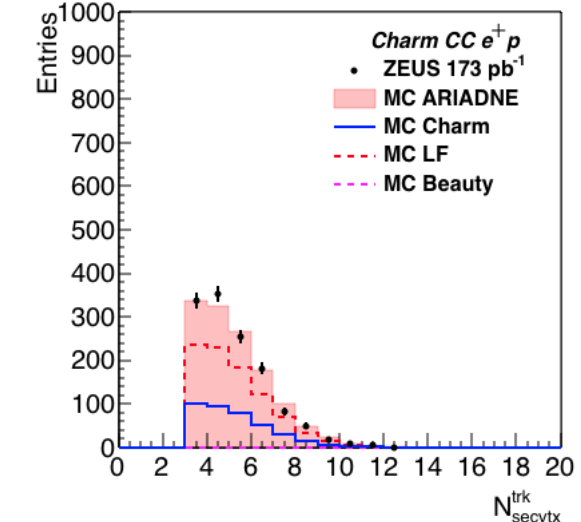
ZEUS



ZEUS

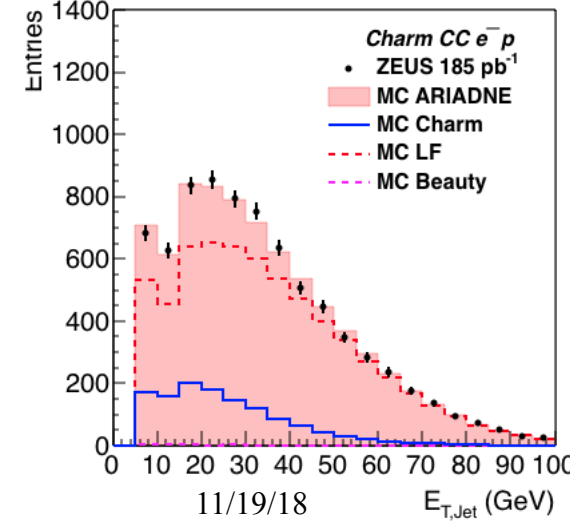


ZEUS

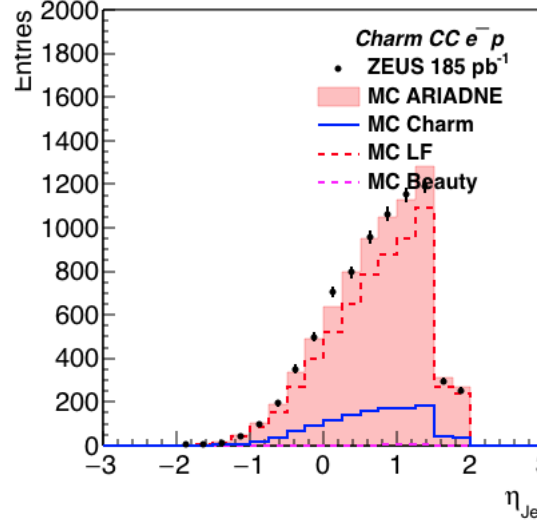


$e^- p$

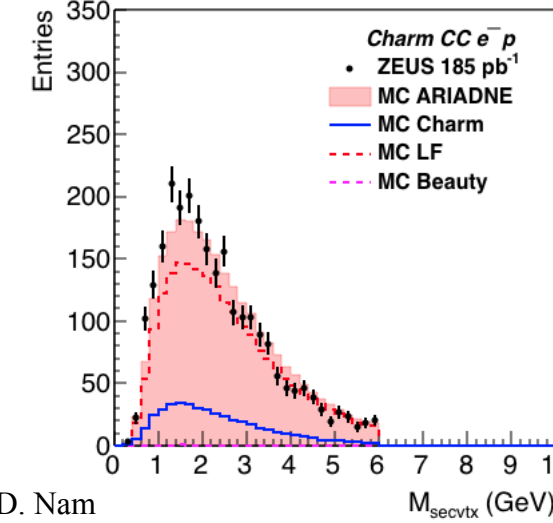
ZEUS



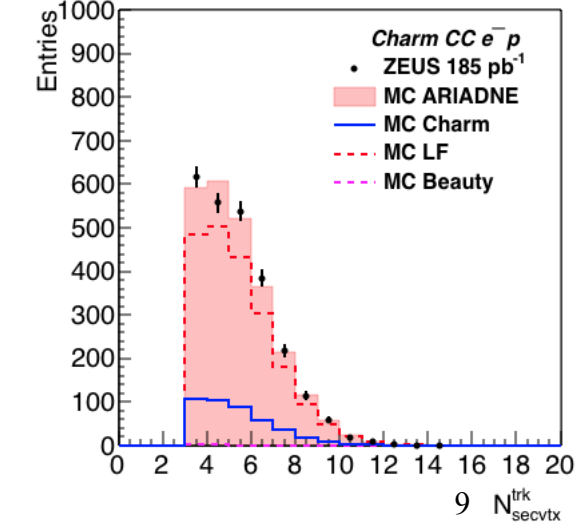
ZEUS



ZEUS



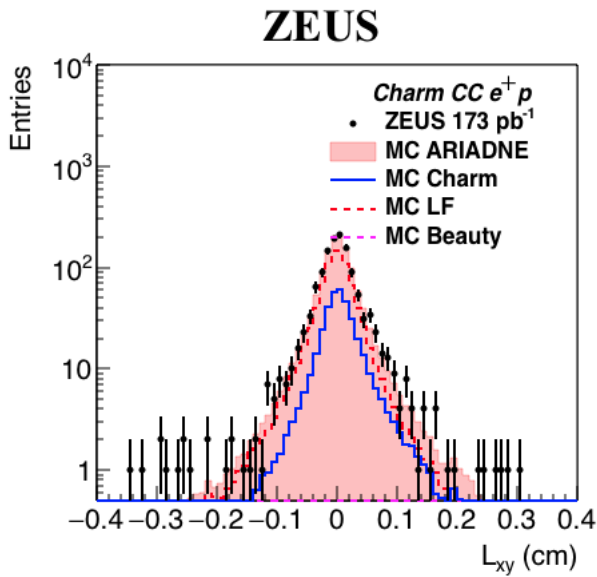
ZEUS



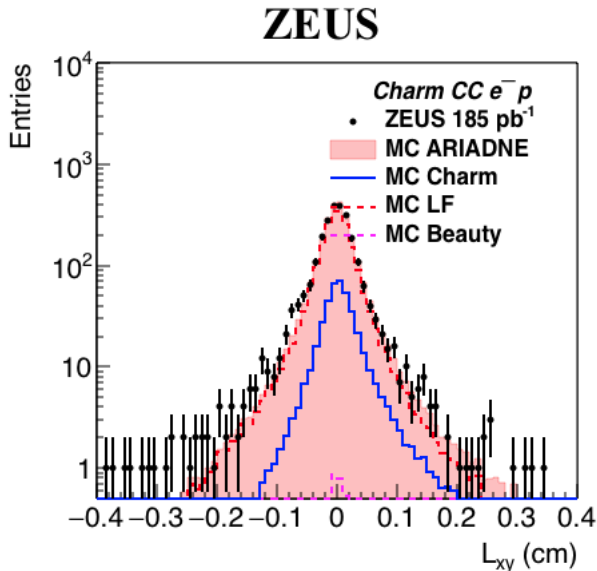
Jae D. Nam

Decay Length Plots

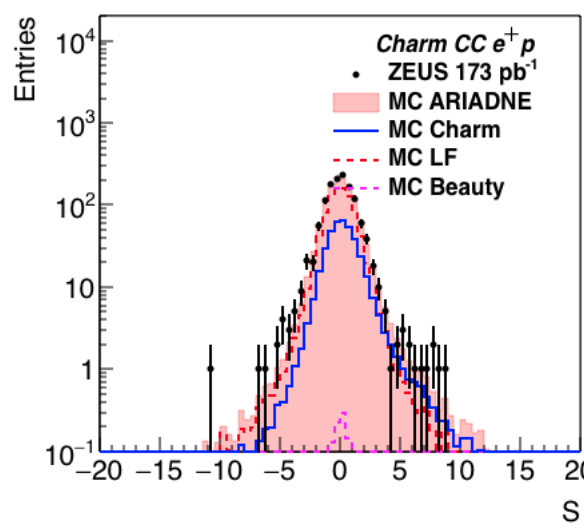
$e^+ p$



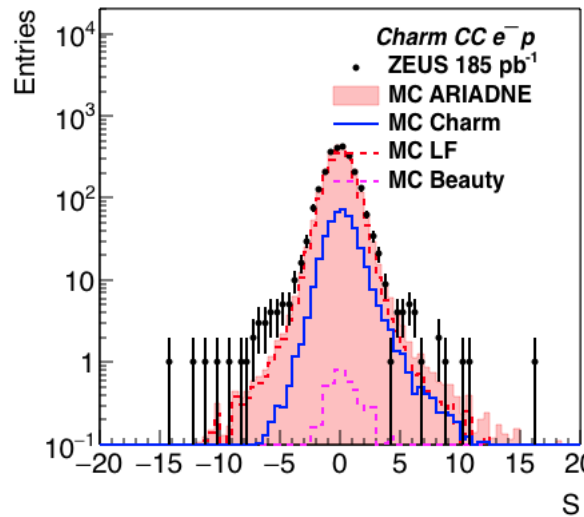
$e^- p$



ZEUS



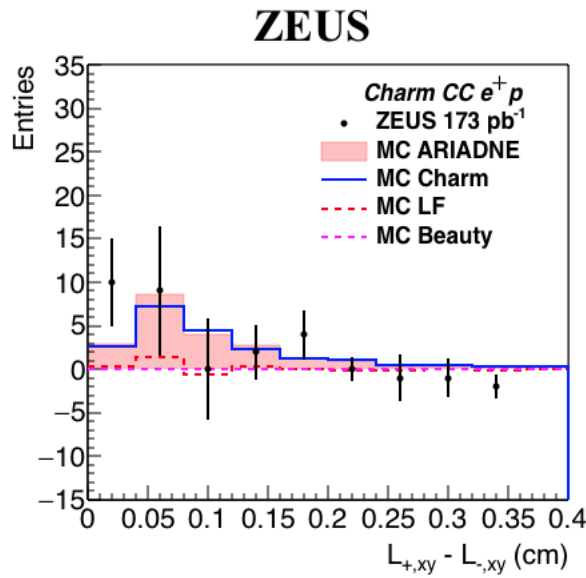
ZEUS



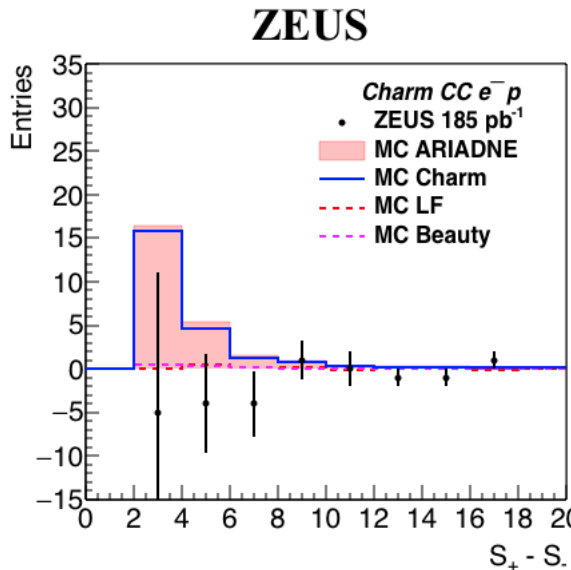
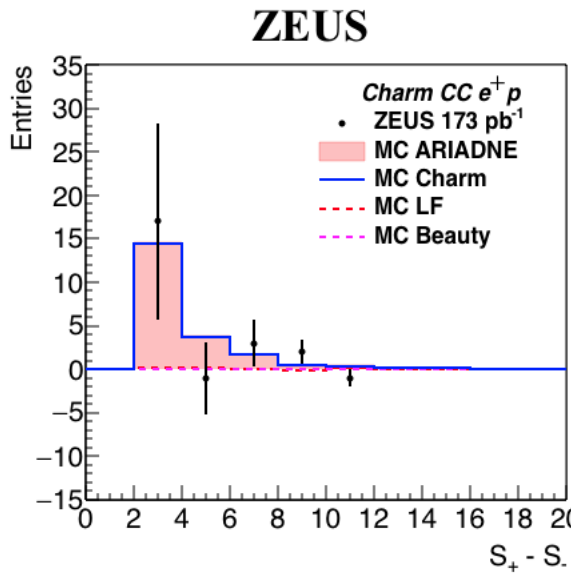
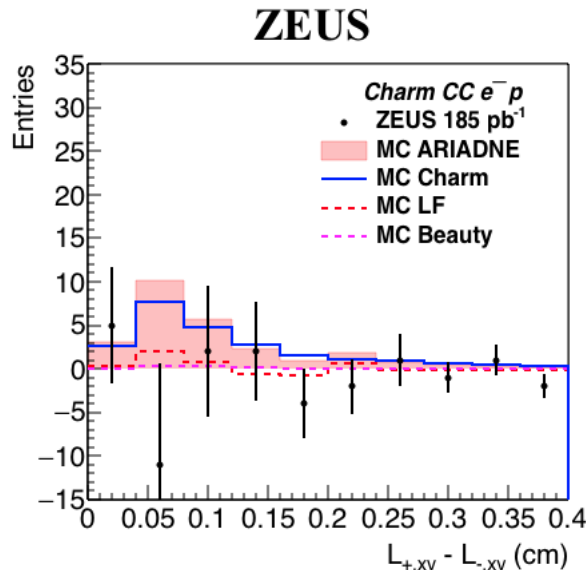
- Asymmetric charm signal observed.
- The high symmetry and large statistics around $S \sim 0$ contributes to a large statistical uncertainty in the low bin regions in $|S|$.
- A significance threshold cut $|S| > 2$ was applied to reduce overall statistical uncertainty.

Mirrored Decay Length

$e^+ p$

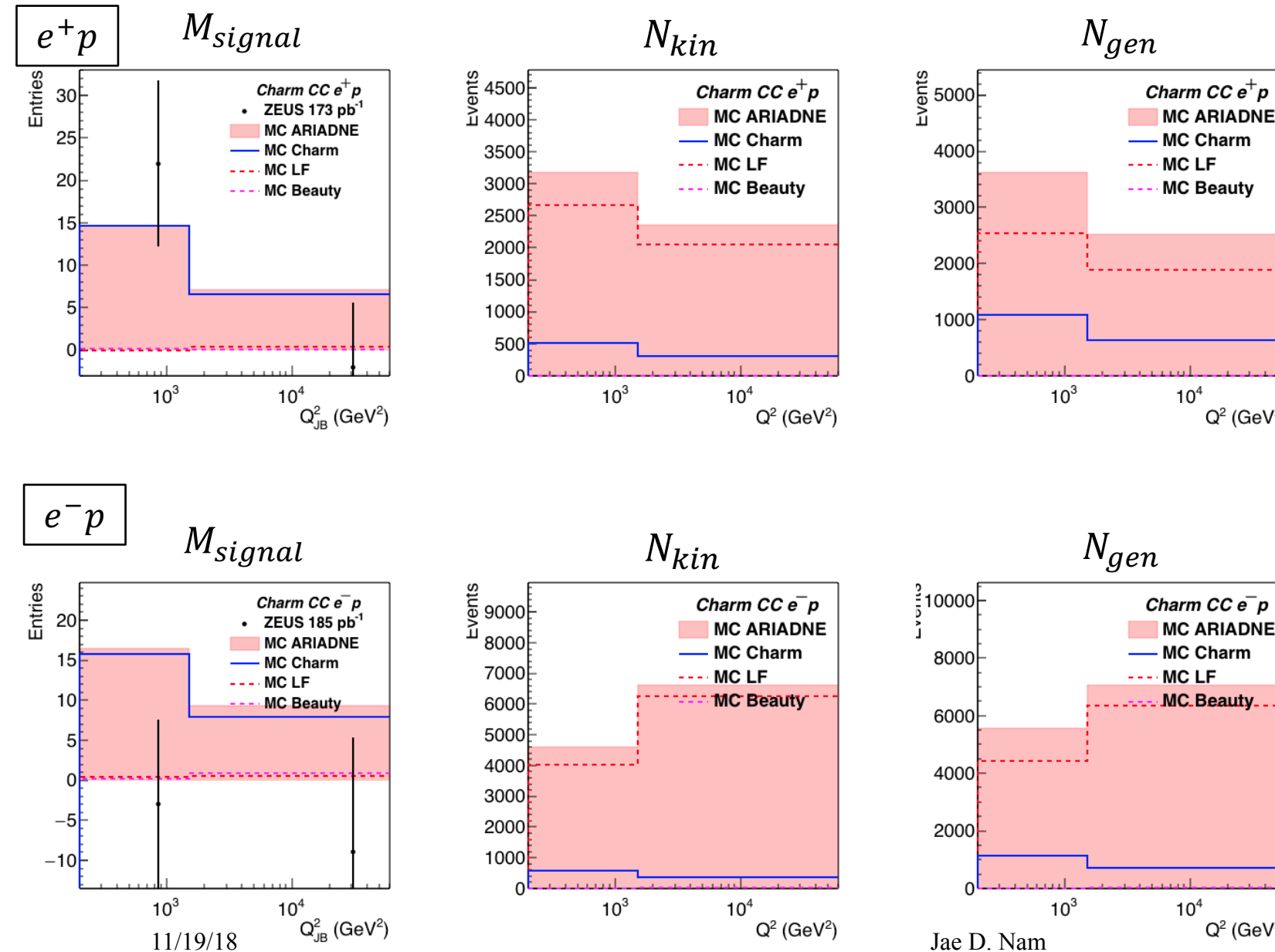


$e^- p$



- Significance cut applied at $|S| > 2$.
- Charm signal observed with LF contribution (Background) suppressed.
- Surviving events are split into 2 bins in Q^2 to unfold charm production cross section, $\sigma_{charm,CC}$.

Charm signal & Charm generated



- N_{gen} = # of events generated in the MC.

- N_{kin} = # of jets associated with charm quark by $\sqrt{\Delta\phi^2 + \Delta\eta^2} < 1$.
 - $\Delta q = q^{jet} - q^{charm}$
 - At the moment, Mc_jet variables are used. Suggestions?

- Visible charm cross section:

$$\sigma_{c,vis} = \frac{M^{DATA} - M_{bg}^{MC}}{M_{charm}^{MC}} \frac{N_{kin}^{MC}}{L}$$

- Visible EW charm cross section:

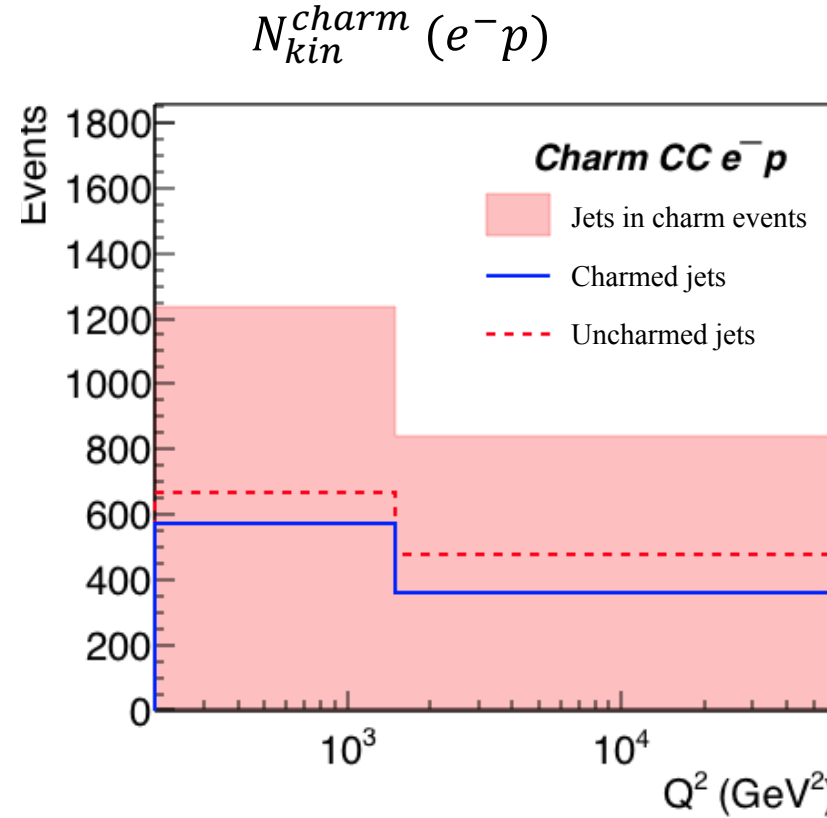
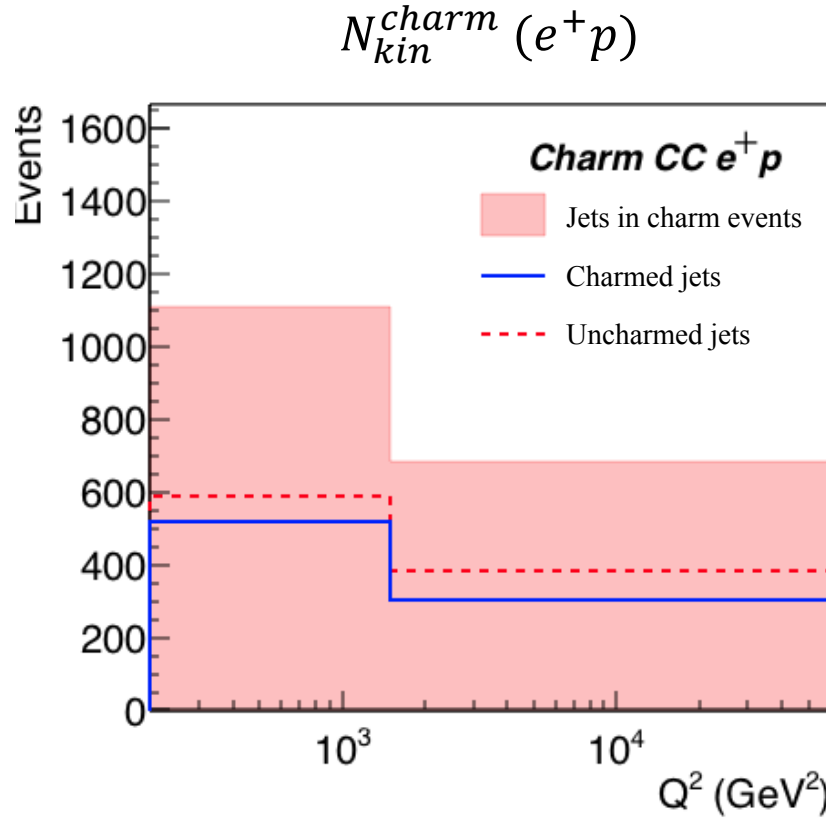
$$\sigma_{c^{EW},vis} = \frac{N_{EW,kin}^{MC}}{N_{kin}^{MC}} \sigma_{c,vis}$$

- Absolute EW charm cross section:

$$\sigma_{c^{EW}} = \frac{N_{EW,gen}^{MC}}{N_{EW,kin}^{MC}} \sigma_{c^{EW},vis}$$

Jae D. Nam

Jets in charm events



- Distributions of generated jets in charmed events within the kinematic range.
 - Jets in charm events = All jets in charm events.
 - Charmed jets = Jets that are associated with charm tracks via $\sqrt{\Delta\phi^2 + \Delta\eta^2} < 1$ where $\Delta q = q^{jet} - q^{charm}$.
 - Uncharmed jets = the ones that are not associated with charm tracks.
 - Mc_jet variables were used to produce these pictures (suggestions welcome!)

Charm signal & Charm generated

Year	Bin	N_{kin}^{EW}	N_{kin}	N_{gen}^{EW}	N_{kin}^{EW}/N_{kin}	$C_{ext,i}$	C_{ext}
0304p	1	101	105	230	0.96	2.28	
	2	55	60	129	0.92	2.34	
	1+2	156	165	359	0.94	2.30	
	Full space			468			3.00
05e	1	390	412	772	0.95	1.98	
	2	202	260	419	0.78	2.07	
	1+2	592	672	1190	0.88	2.01	
	Full space			1563			2.64
06e	1	149	158	304	0.95	2.03	
	2	77	100	166	0.77	2.16	
	1+2	226	258	470	0.88	2.08	
	Full space			619			2.74
0607p	1	396	414	819	0.96	2.07	
	2	220	240	463	0.91	2.11	
	1+2	615	654	1282	0.94	2.08	
	Full space			1677			2.72

- Full space:
 $Q^2 < 200 \text{ GeV}^2 \text{ } \&\& \text{ } Q^2 > 60000 \text{ GeV}^2$
- $C_{ext,i} = N_{gen,i}^{EW}/N_{kin,i}^{EW}$
where i runs over for bin 1, 2 and 1+2.
- $C'_{ext} = N_{gen,full}^{EW}/N_{kin,1+2}^{EW}$

Systematic Uncertainties

Sources	Variable	Variation	$\delta\sigma_{c^{EW}}^+$	$\delta\sigma_{c^{EW}}^-$
DIS selection			Negligible ($\sim 2\%$)	Negligible ($\sim 2\%$)
Secondary Vertex selection	N_{secvtx}^{trk}	> 1	+1.9 pb	+3.5 pb
Calorimeter	E_T	$\pm 3\%$	Negligible ($< 1\%$)	Negligible ($< 1\%$)
LF background	N_{LF}	$\pm 30\%$	Negligible ($< 1\%$)	Negligible ($\sim 2\%$)
QCD charm fraction	$\frac{N_{QCD}}{N_{charm}}$	$\pm 100\%$	∓ 0.42 pb	± 0.64 pb
Rescaling			-1.6 pb	+1.1 pb
Signal Extraction	S_{thresh}	± 1	± 6.2 pb	± 3.9 pb
Total			+6.5 pb	+5.4 pb
			-6.4 pb	-3.9 pb

δ_1 DIS Selection & Secondary vertex selection

- Uncertainty associated with the selection threshold values.

δ_2 Calorimeter

- Due to imperfect calibration of hadronic calorimeter (HAC). Uncertainty in E_T^{jet} is known to be $\pm 3\%$.

δ_3 Background

- Asymmetry in LF decay length due to long-lived LF particles.

δ_4 QCD charm fraction in MC

- Uncertainty associated with the QCD charm fraction calculated in MC is tested by varying the fraction by $\pm 100\%$.

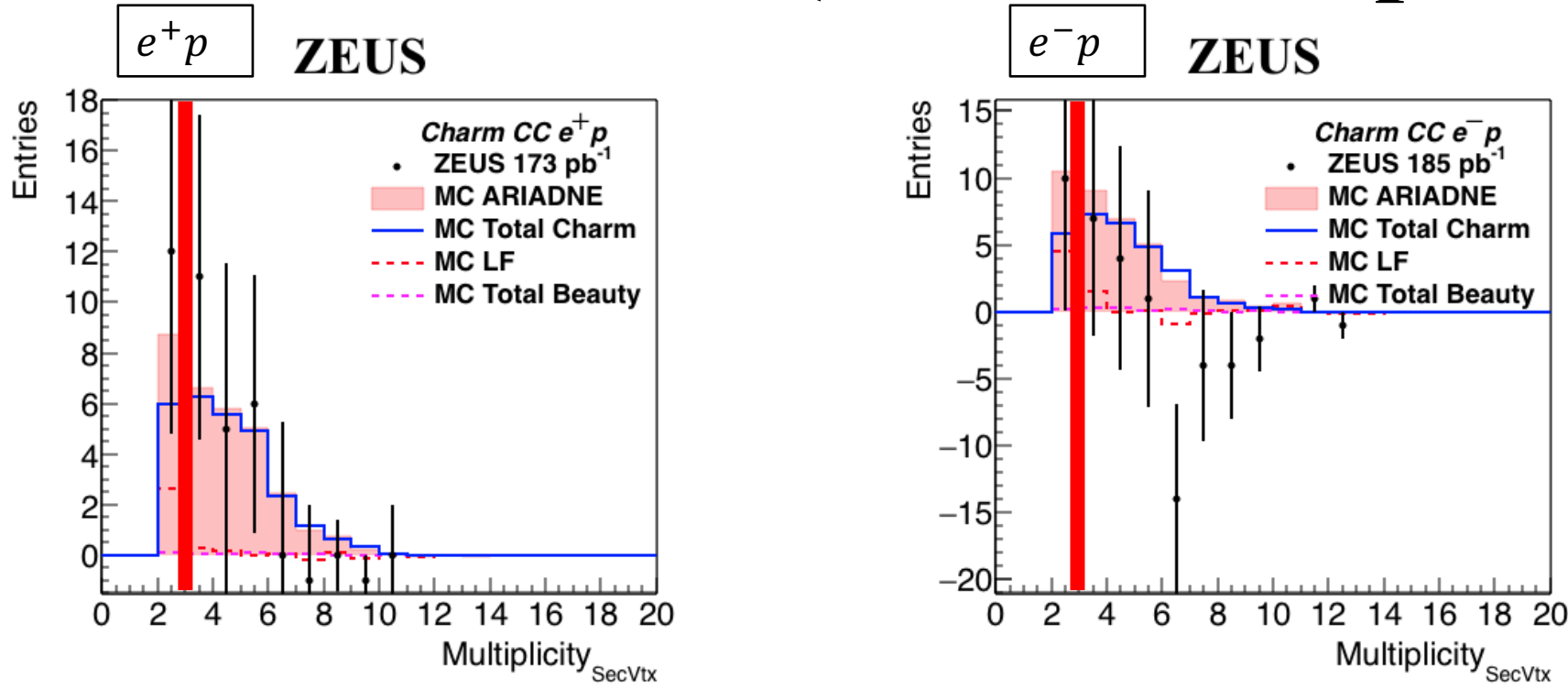
δ_4 Secondary Vertex Rescaling

- More secondary vertices survive in MC than in data. Rescaling was only applied to the light-flavor signal to account for different causes of the discrepancy.

δ_5 Signal Extraction

- Due to the low statistics & high fluctuation in data, further study will be performed.

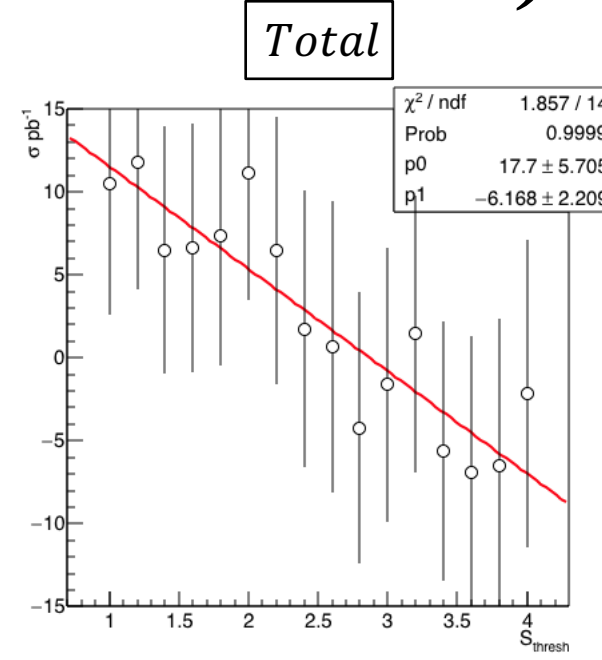
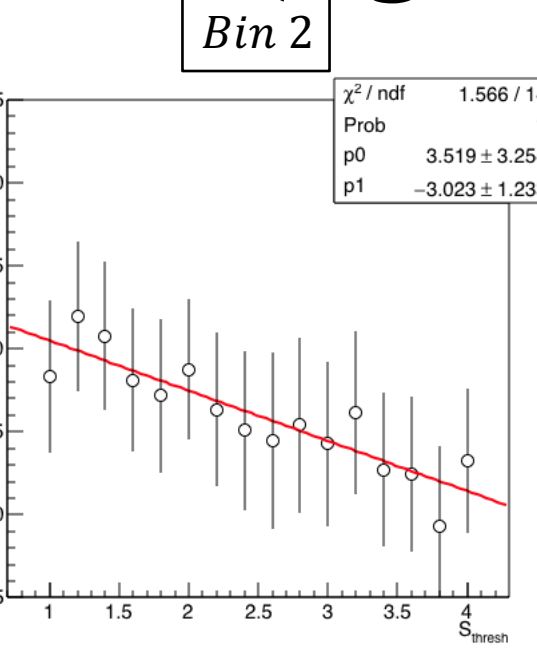
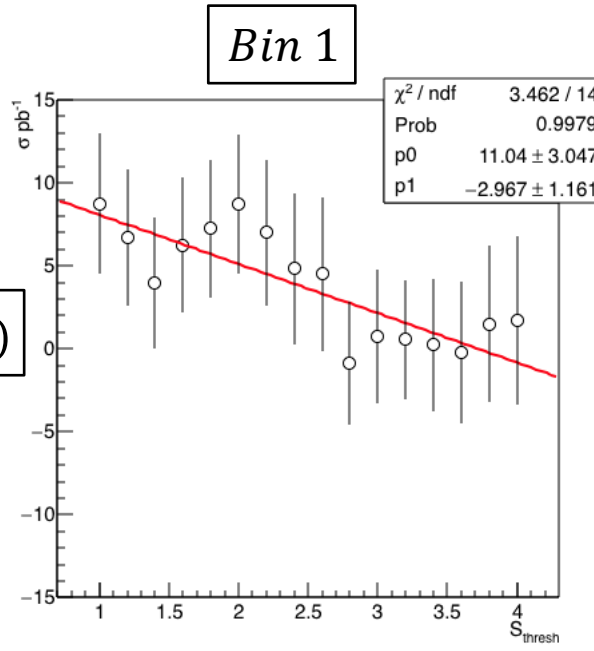
Systematic uncertainties (secvtx multiplicity)



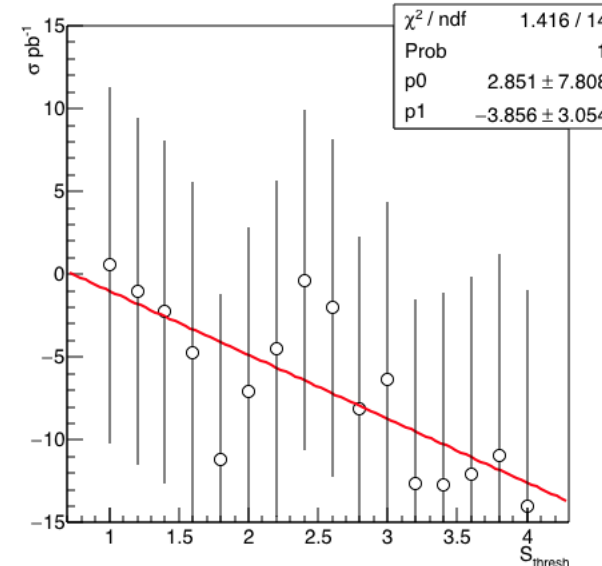
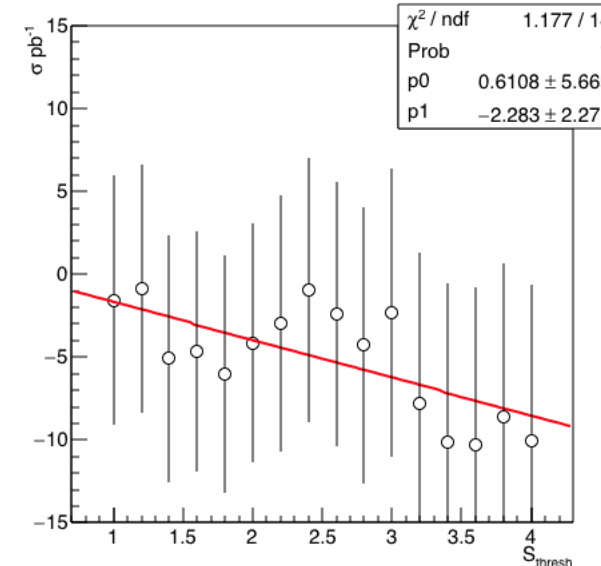
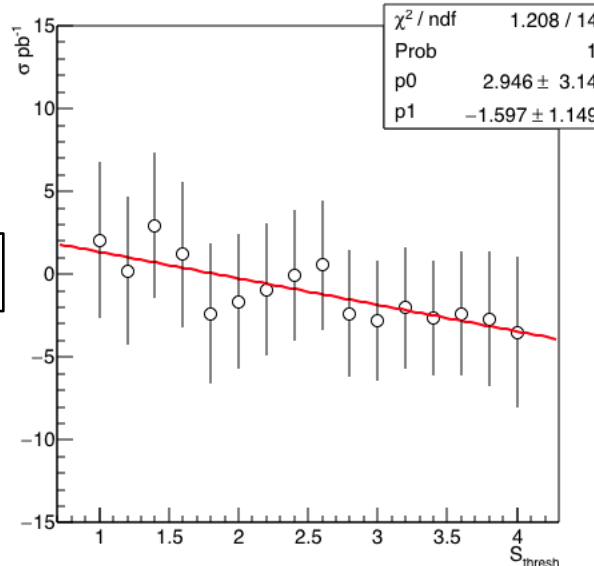
- Multiplicity distribution after signal extraction.
- The red vertical bars represent the selection cut. The distributions on the right of the bar are the "nominal" distribution.
- The uncertainty associated with this cut is determined by including the distribution left of the bar.

Systematic uncertainties (signal extraction)

$\sigma^{e^+p}(S_{\text{thresh}})$



$\sigma^{e^-p}(S_{\text{thresh}})$

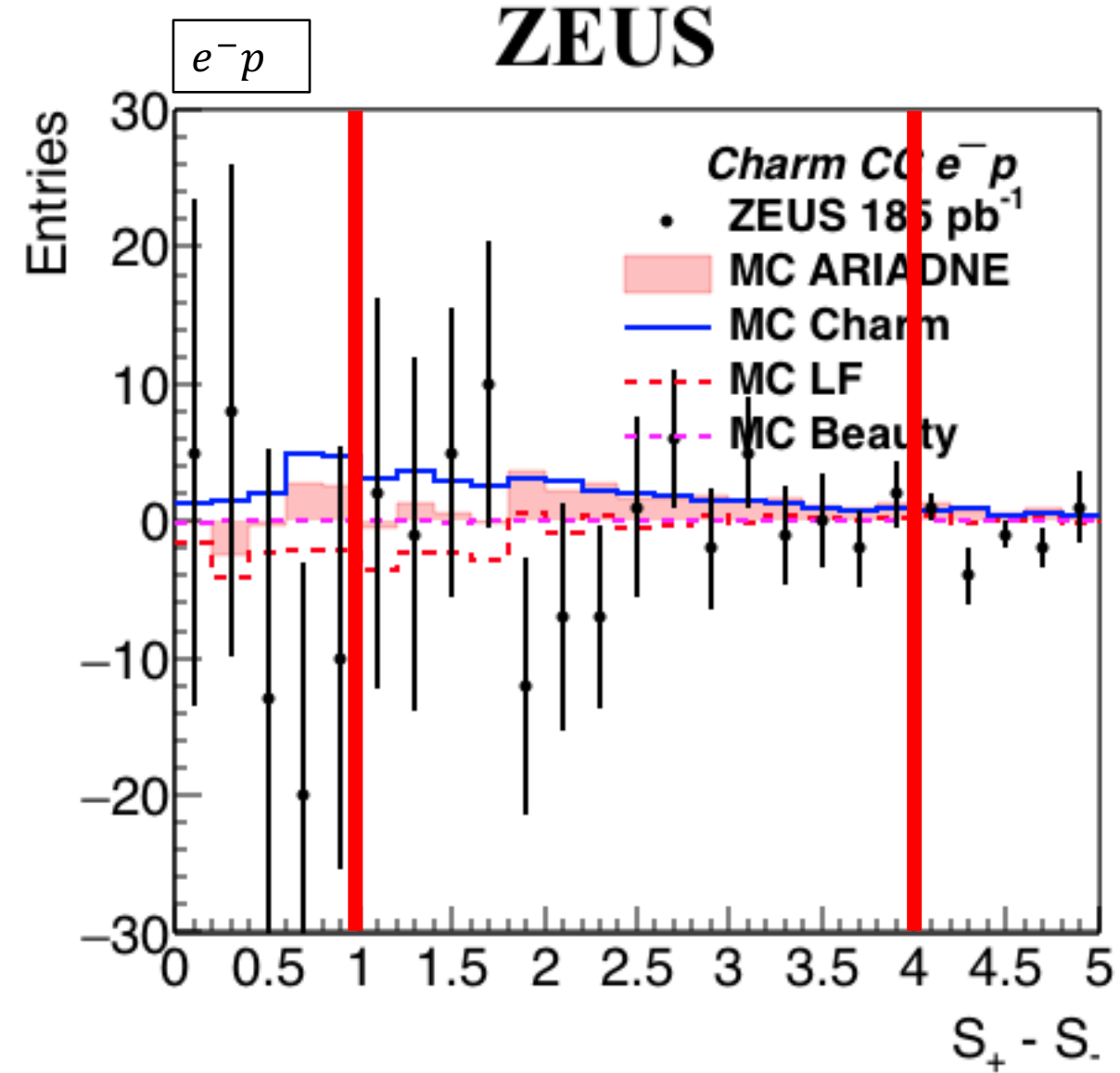
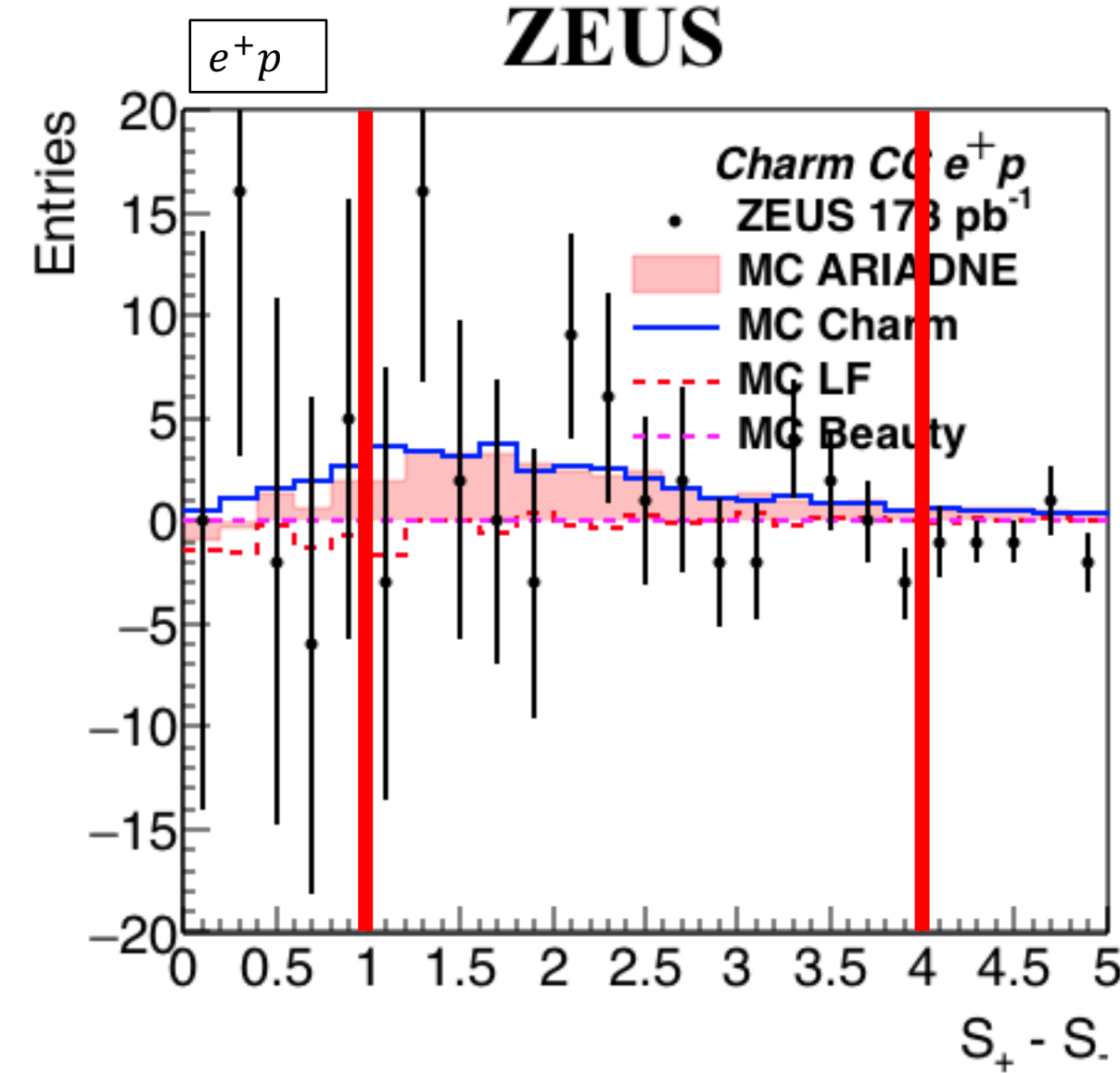


11/19/1

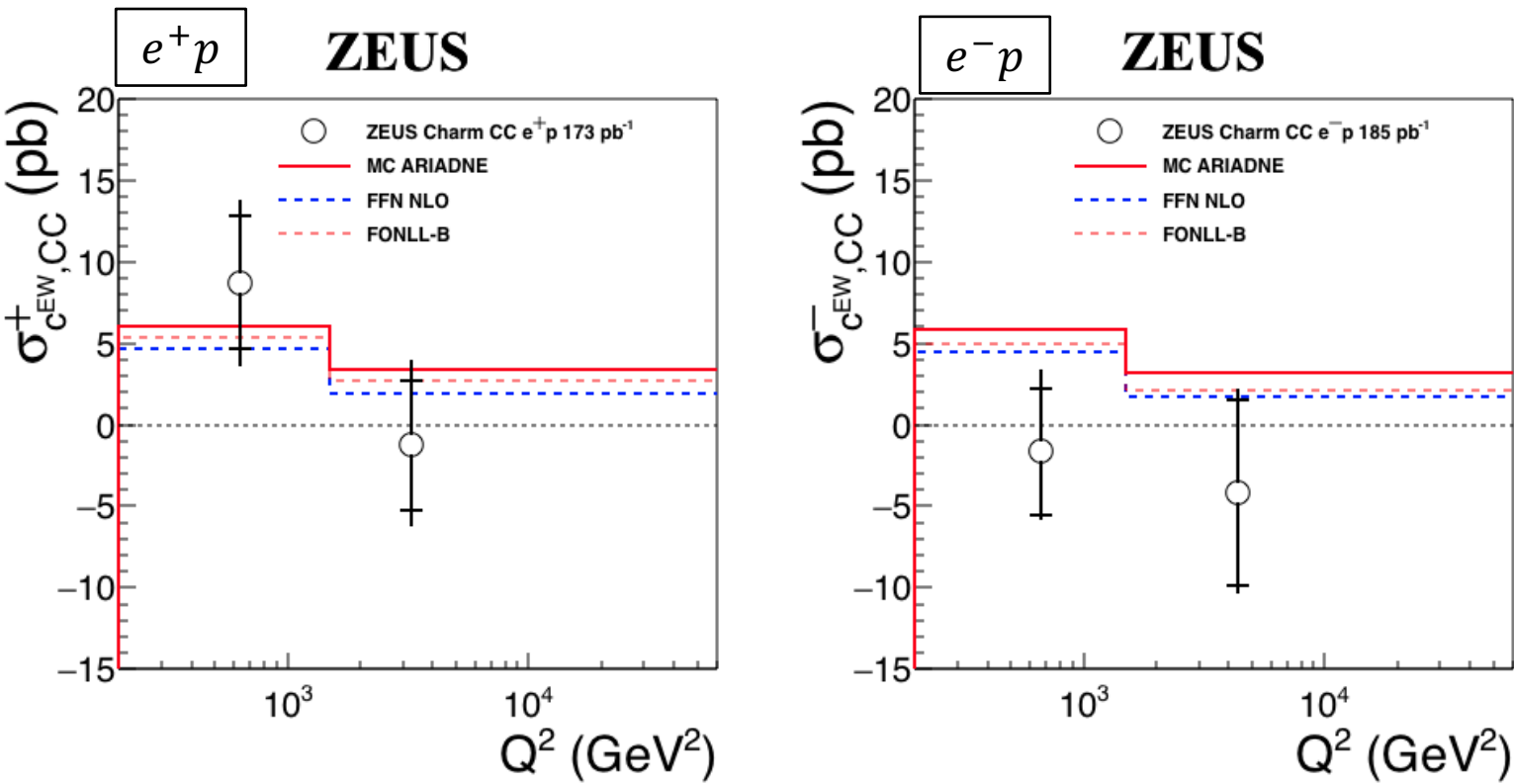
17



Mirrored significance distribution



Results



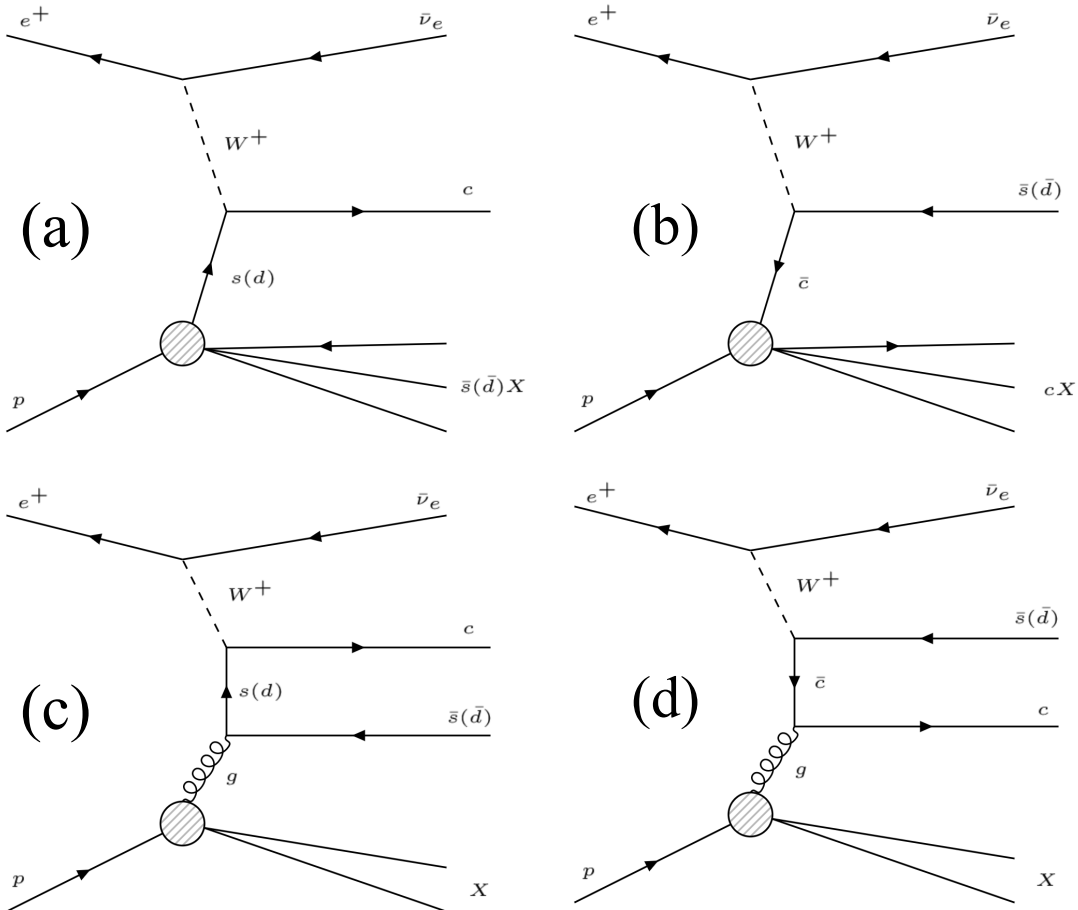
- 0304p & 0607p, 05e & 06e combined at the cross section level.
- (preliminary method) Total EW charm cross sections are measured to be

$$\sigma_{c^{EW}}^+ = 11.1 \pm 7.3 \text{ (stat)} {}^{+6.5}_{-6.4} \text{ (syst) pb}$$

$$\sigma_{c^{EW}}^- = -7.1 \pm 8.8 \text{ (stat)} {}^{+5.4}_{-3.9} \text{ (syst) pb}$$

- FFN scheme:
 - ABMP16.3 NLO pdf set, OPENQCDRAD
- FONLL scheme:
 - NNPDF31 NLO pdf set, APFEL
- Both are interfaced in xFitter.

Theory predictions & recap of charm subprocesses



	$d \rightarrow c$	$s \rightarrow c$	$\bar{c} \rightarrow \bar{s}/\bar{d}$
MC	(a) + (c)	(a) + (c)	(b) + (d)
FFN	(a) + (c)	(a) + (c)	(d) w/ larger gluon content
FONLL	(a) + (c)	(a) + (c)	(b) + (d)

$e^+ p$	$200 < Q^2 < 1500 \text{ GeV}^2$			
	$\sigma_{c\text{EW}}(\text{ pb})$	$d \rightarrow c(\%)$	$s \rightarrow c(\%)$	$\bar{c} \rightarrow \bar{s}/\bar{d}$
MC	6.07 ± 0.29	6	36	58
FFN NLO	4.72 ± 0.05	8	49	43
FONLL-B	5.37 ± 0.21	8	43	50
$e^+ p$	$1500 < Q^2 < 60000 \text{ GeV}^2$			
	$\sigma_{c\text{EW}}(\text{ pb})$	$d \rightarrow c(\%)$	$s \rightarrow c(\%)$	$\bar{c} \rightarrow \bar{s}/\bar{d}$
MC	3.42 ± 0.32	10	26	64
FFN NLO	1.97 ± 0.03	16	43	41
FONLL-B	2.66 ± 0.23	12	37	51
$e^- p$	$200 < Q^2 < 1500 \text{ GeV}^2$			
	$\sigma_{c\text{EW}}(\text{ pb})$	$\bar{d} \rightarrow \bar{c}(\%)$	$\bar{s} \rightarrow \bar{c}(\%)$	$c \rightarrow s/d$
MC	5.81 ± 0.40	3	37	60
FFN NLO	4.50 ± 0.05	4	51	45
FONLL-B	4.98 ± 0.22	4	43	54
$e^- p$	$1500 < Q^2 < 60000 \text{ GeV}^2$			
	$\sigma_{c\text{EW}}(\text{ pb})$	$\bar{d} \rightarrow \bar{c}(\%)$	$\bar{s} \rightarrow \bar{c}(\%)$	$c \rightarrow s/d$
MC	3.16 ± 0.52	2	29	69
FFN NLO	1.73 ± 0.03	5	49	46
FONLL-B	2.16 ± 0.22	4	33	63

Requested for Paper

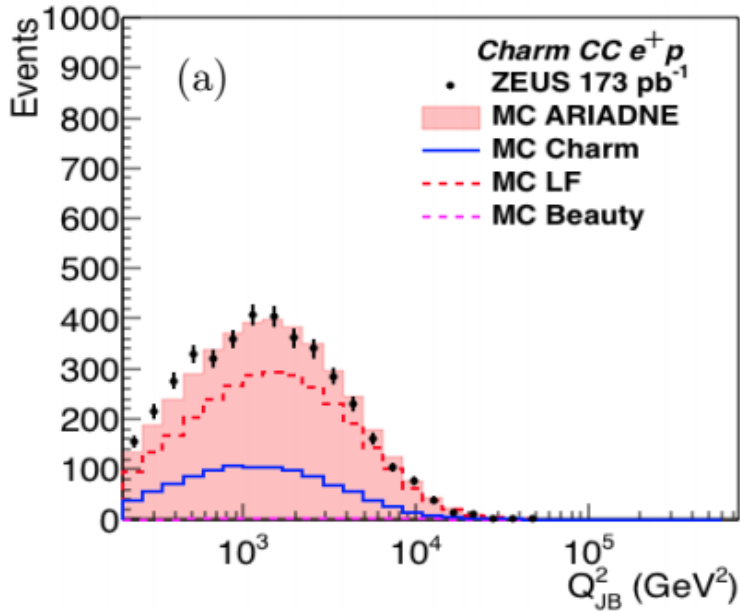
Q^2 range (GeV 2)	$\sigma_{c,\text{vis}}(\text{ pb})$			
e^+p				
200–1500	4.1	± 2.0	(stat.)	$^{+1.5}_{-1.6}$ (syst.)
1500–60000	-0.7	± 2.0	(stat.)	$^{+1.7}_{-1.5}$ (syst.)
e^-p				
200–1500	-0.9	± 2.1	(stat.)	$^{+1.6}_{-0.9}$ (syst.)
1500–60000	-2.6	± 3.5	(stat.)	$^{+1.5}_{-1.4}$ (syst.)
Q^2 range (GeV 2)	$\sigma_{c^{\text{EW}},\text{vis}}(\text{ pb})$			
e^+p				
200–1500	3.9	± 1.9	(stat.)	$^{+1.5}_{-1.6}$ (syst.)
1500–60000	-0.6	± 1.8	(stat.)	$^{+1.5}_{-1.4}$ (syst.)
e^-p				
200–1500	-0.8	± 1.9	(stat.)	$^{+1.5}_{-0.8}$ (syst.)
1500–60000	-2.0	± 2.7	(stat.)	$^{+1.3}_{-1.2}$ (syst.)
Q^2 range (GeV 2)	$\sigma_{c^{\text{EW}}}(\text{ pb})$			
e^+p				
200–1500	8.7	± 4.1	(stat.)	$^{+3.0}_{-3.3}$ (syst.)
1500–60000	-1.2	± 4.0	(stat.)	$^{+3.4}_{-3.0}$ (syst.)
e^-p				
200–1500	-1.6	± 3.8	(stat.)	$^{+2.9}_{-1.6}$ (syst.)
1500–60000	-4.2	± 5.7	(stat.)	$^{+2.6}_{-2.5}$ (syst.)

Requested for Paper

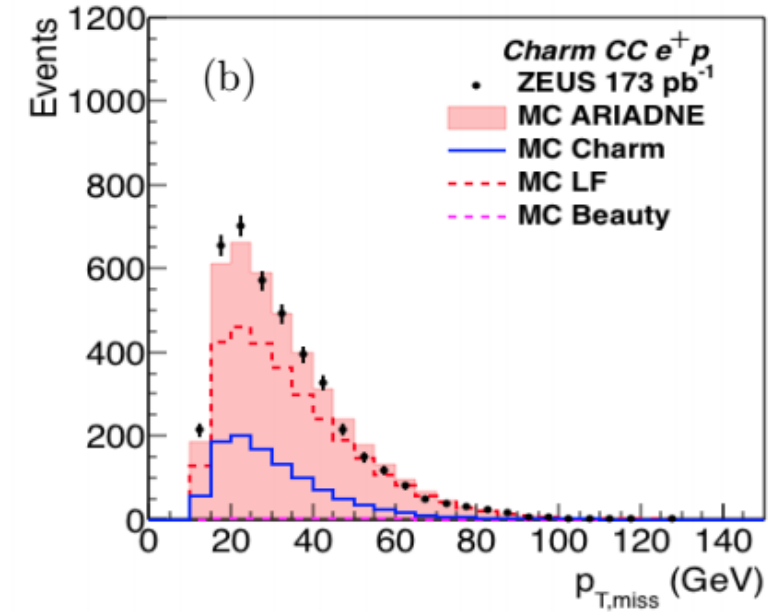
$e^+ p$	200 < Q^2 < 1500 GeV 2			
	$\sigma_{c\text{EW}}(\text{ pb})$	$d \rightarrow c(\%)$	$s \rightarrow c(\%)$	$\bar{c} \rightarrow \bar{s}/\bar{d}$
MC	6.07 ± 0.29	6	36	58
FFN NLO	4.72 ± 0.05	8	49	43
FONLL-B	5.37 ± 0.21	8	43	50
$e^+ p$	1500 < Q^2 < 60000 GeV 2			
	$\sigma_{c\text{EW}}(\text{ pb})$	$d \rightarrow c(\%)$	$s \rightarrow c(\%)$	$\bar{c} \rightarrow \bar{s}/\bar{d}$
MC	3.42 ± 0.32	10	26	64
FFN NLO	1.97 ± 0.03	16	43	41
FONLL-B	2.66 ± 0.23	12	37	51
$e^- p$	200 < Q^2 < 1500 GeV 2			
	$\sigma_{c\text{EW}}(\text{ pb})$	$\bar{d} \rightarrow \bar{c}(\%)$	$\bar{s} \rightarrow \bar{c}(\%)$	$c \rightarrow s/d$
MC	5.81 ± 0.40	3	37	60
FFN NLO	4.50 ± 0.05	4	51	45
FONLL-B	4.98 ± 0.22	4	43	54
$e^- p$	1500 < Q^2 < 60000 GeV 2			
	$\sigma_{c\text{EW}}(\text{ pb})$	$\bar{d} \rightarrow \bar{c}(\%)$	$\bar{s} \rightarrow \bar{c}(\%)$	$c \rightarrow s/d$
MC	3.16 ± 0.52	2	29	69
FFN NLO	1.73 ± 0.03	5	49	46
FONLL-B	2.16 ± 0.22	4	33	63

Requested for Paper

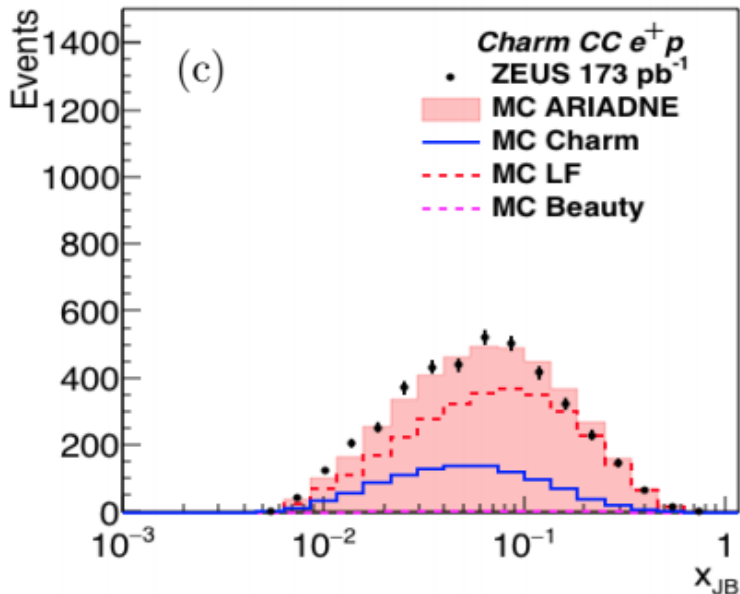
ZEUS



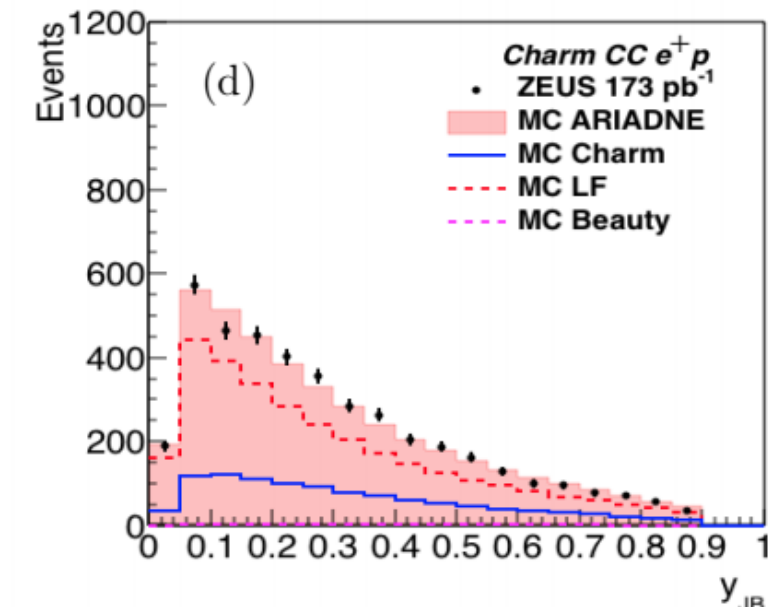
ZEUS



ZEUS

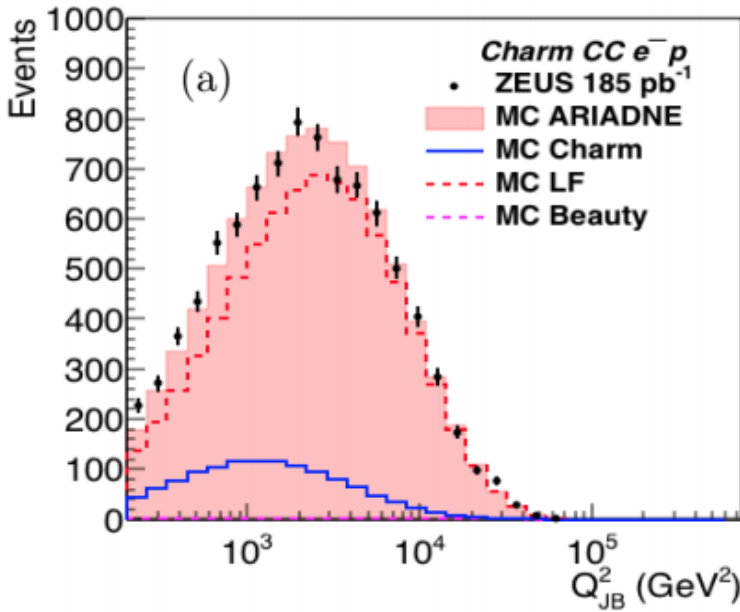


ZEUS

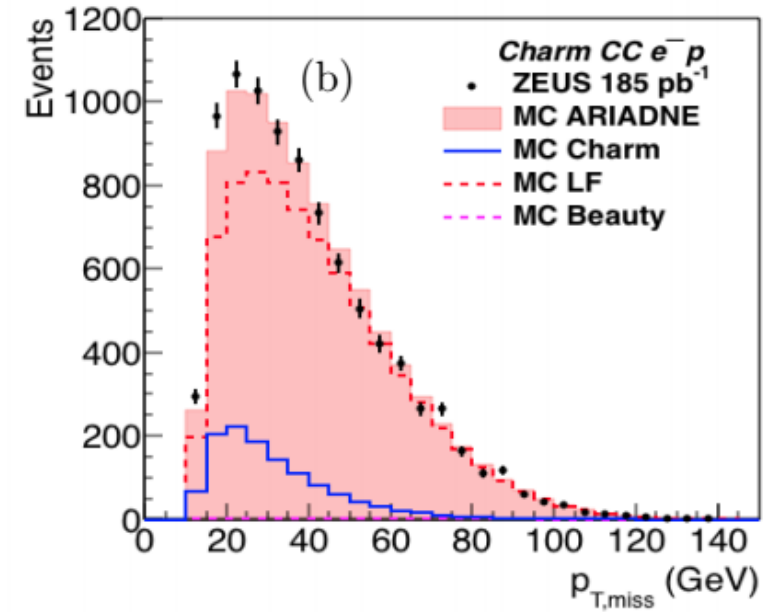


Requested for Paper

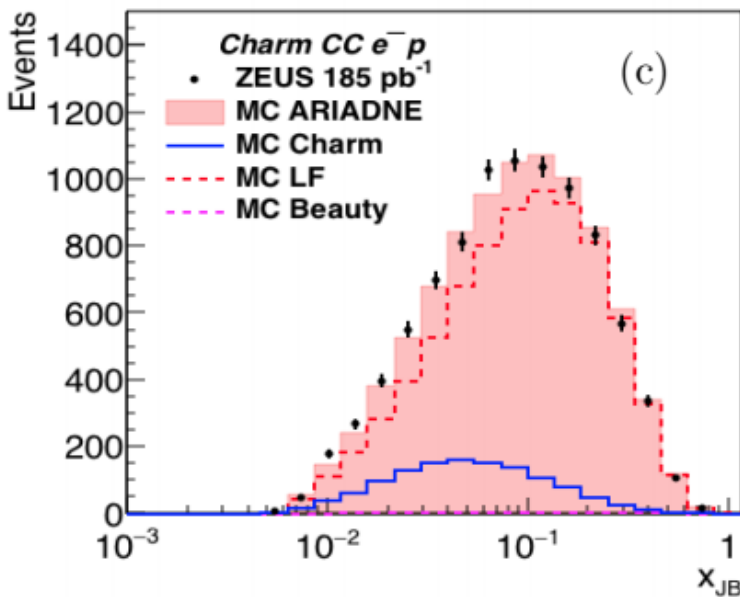
ZEUS



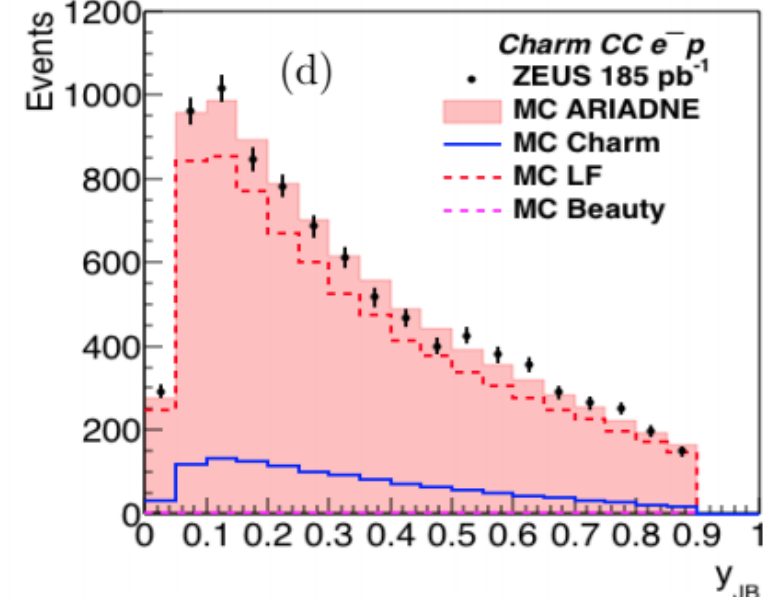
ZEUS



ZEUS

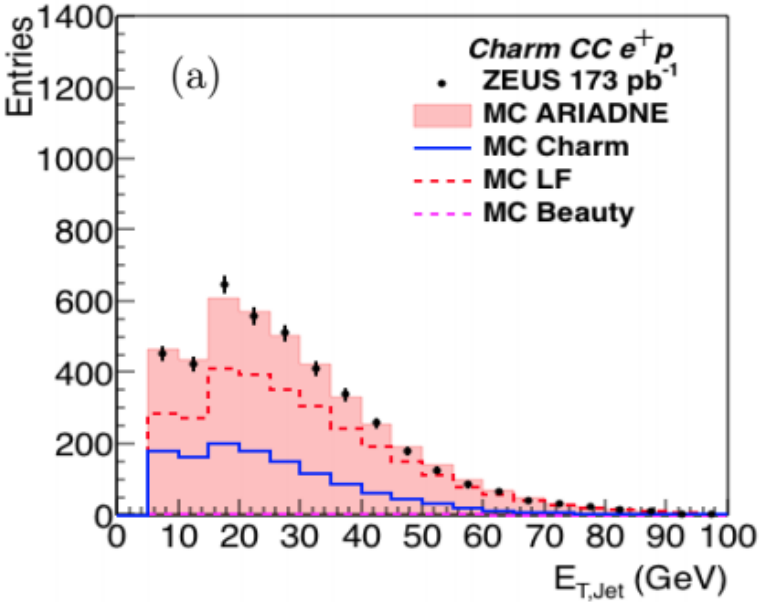


ZEUS

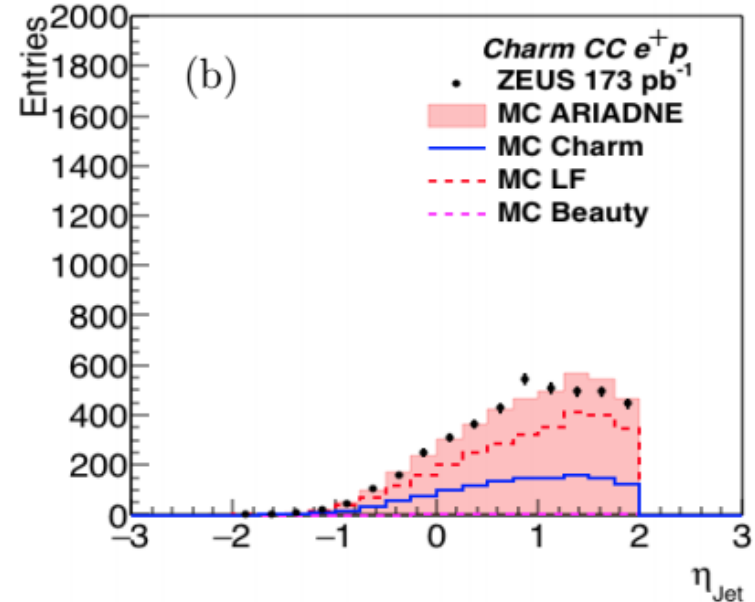


Requested for Paper

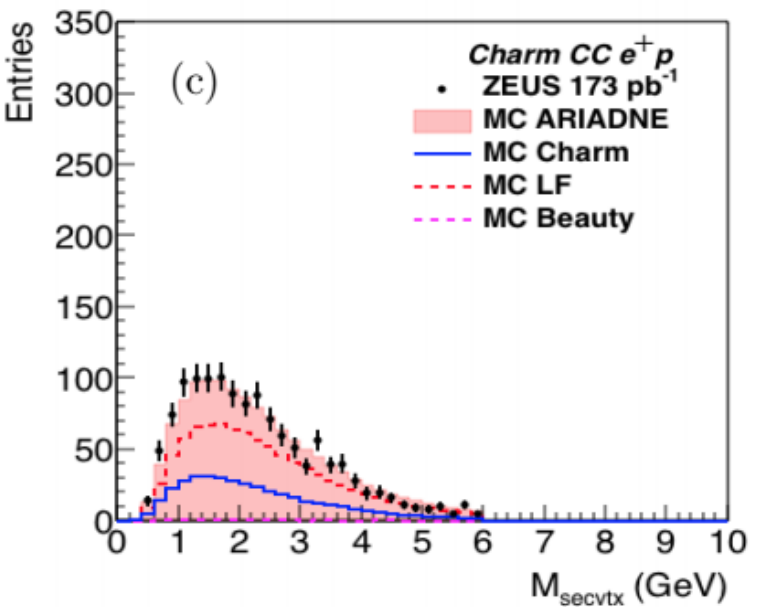
ZEUS



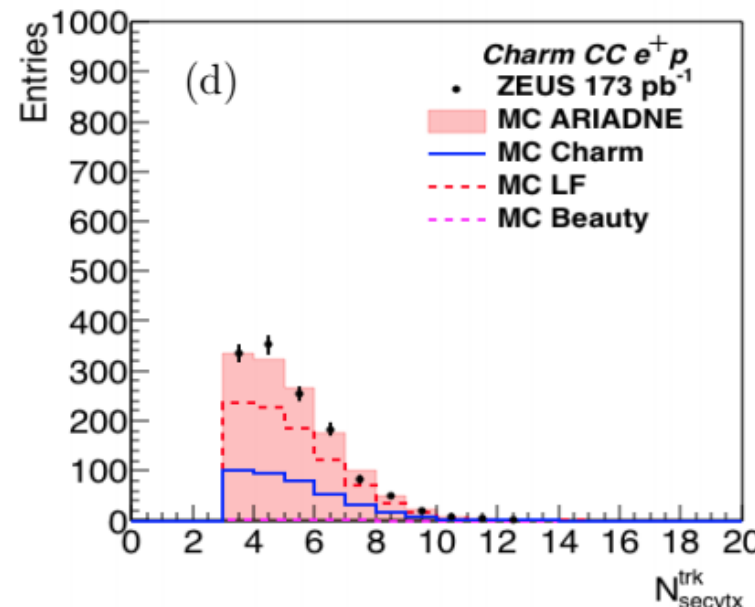
ZEUS



ZEUS

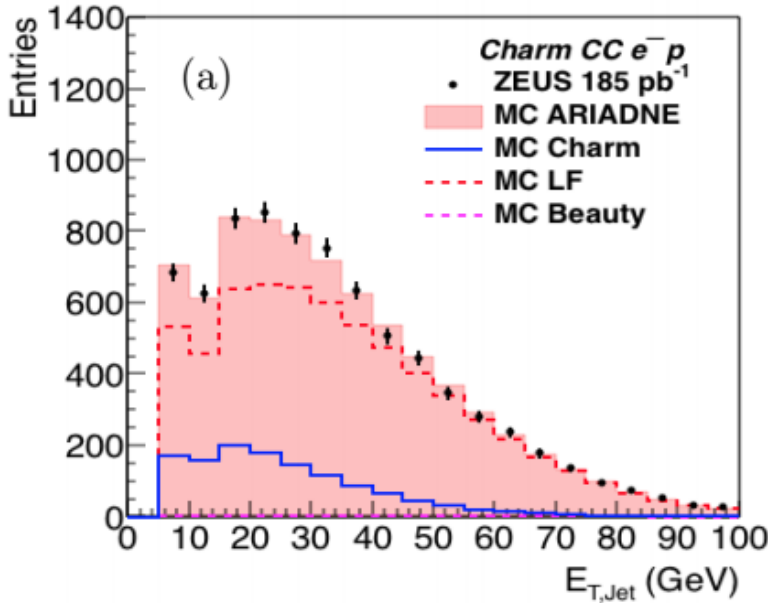


ZEUS

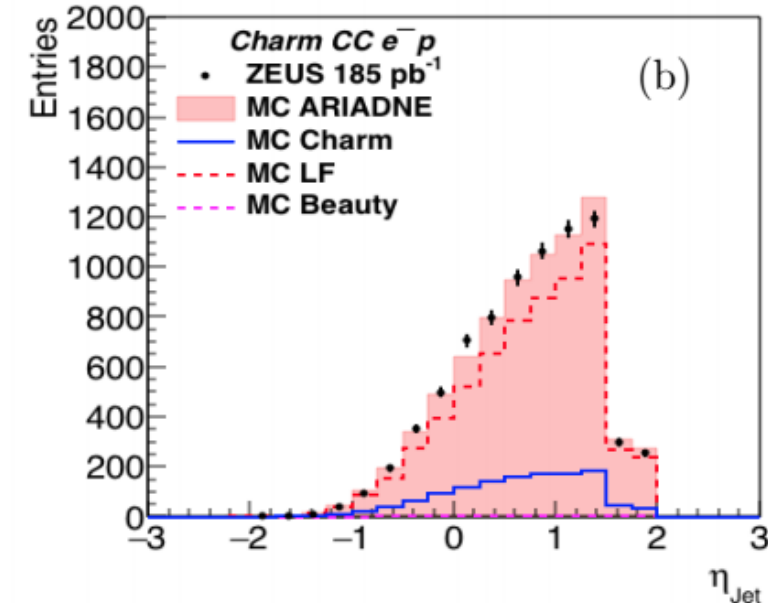


Requested for Paper

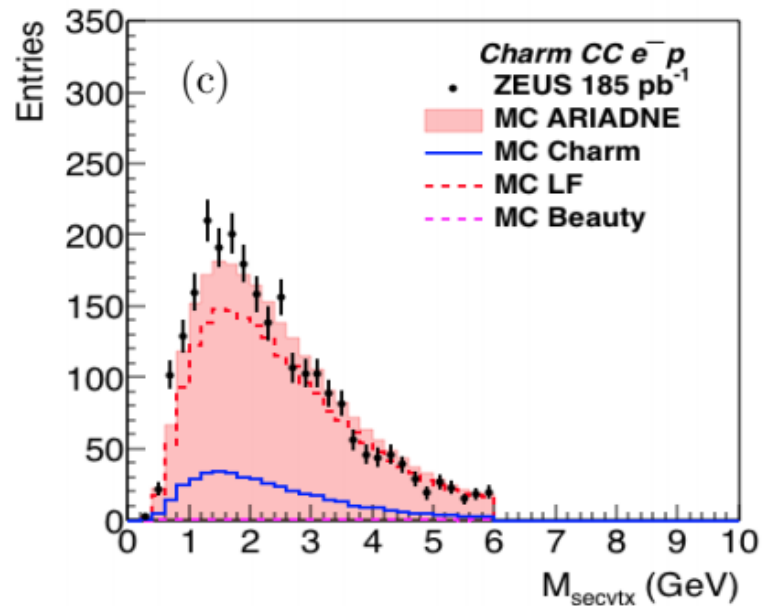
ZEUS



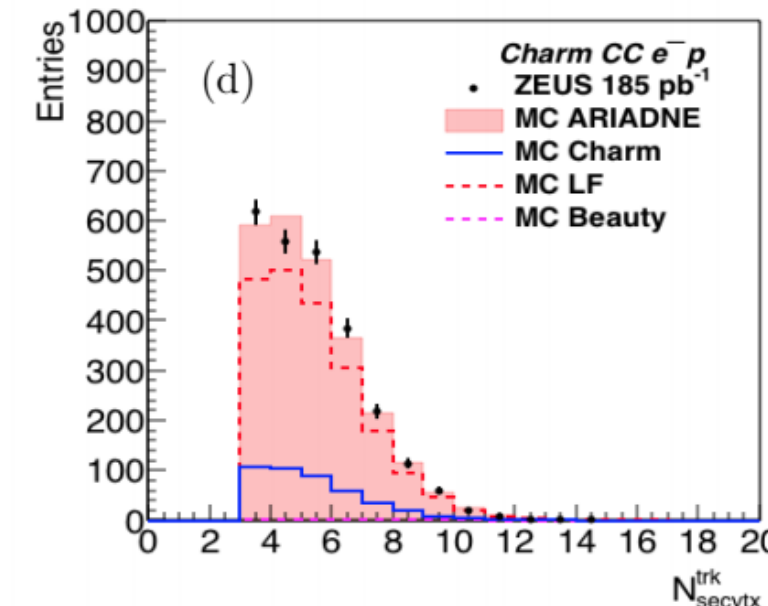
ZEUS



ZEUS

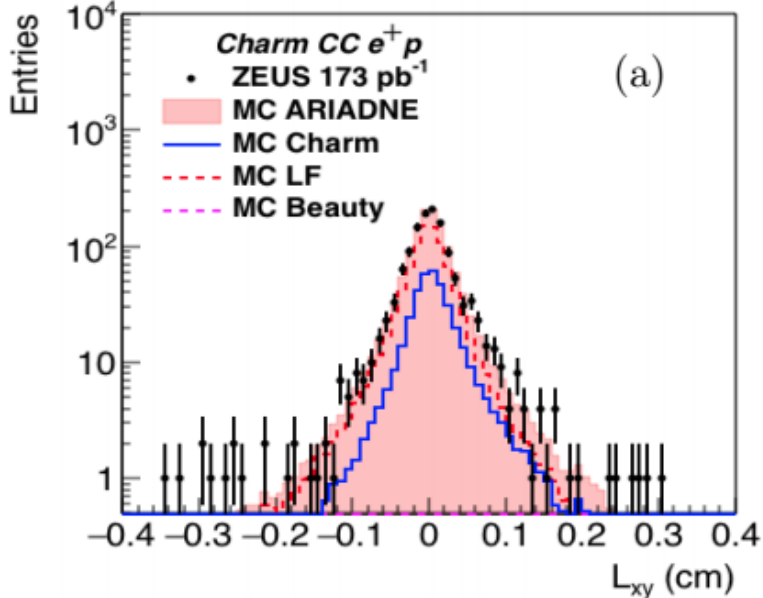


ZEUS

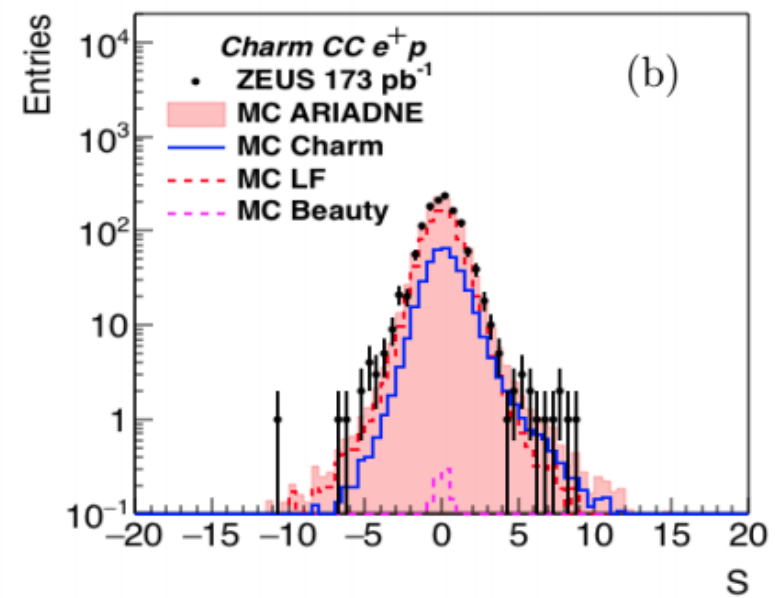


Requested for Paper

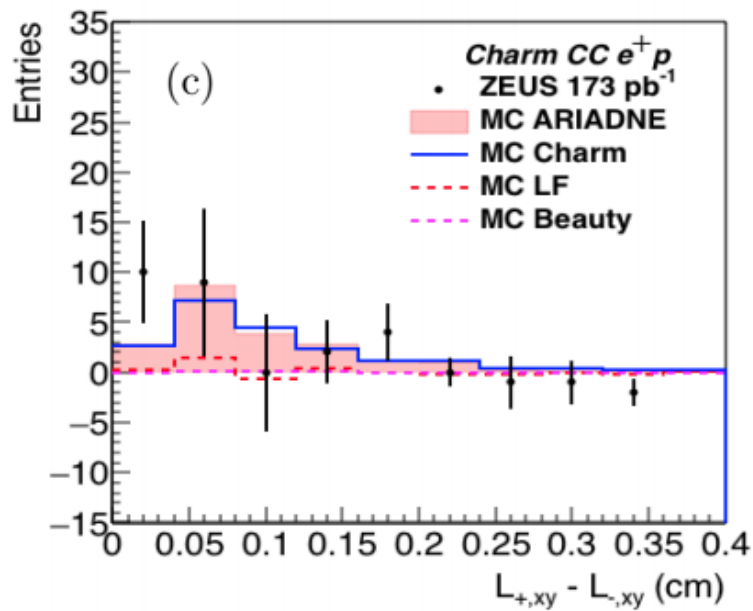
ZEUS



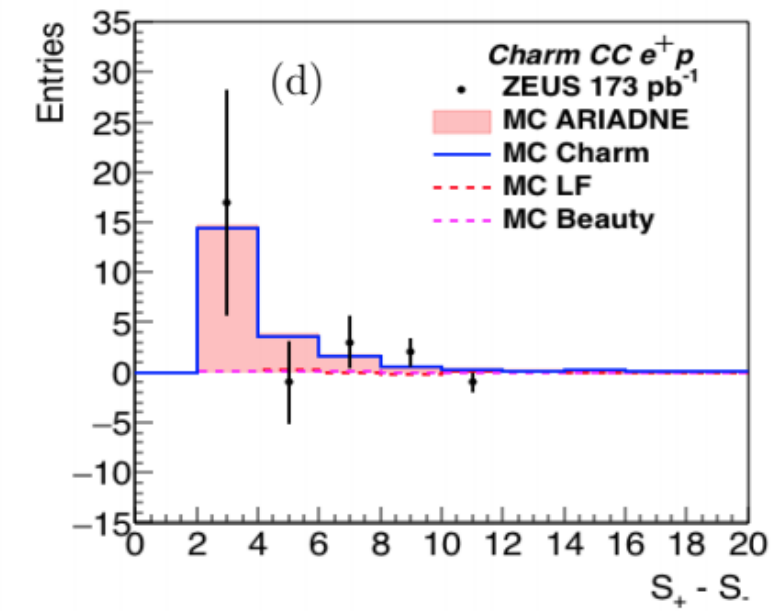
ZEUS



ZEUS

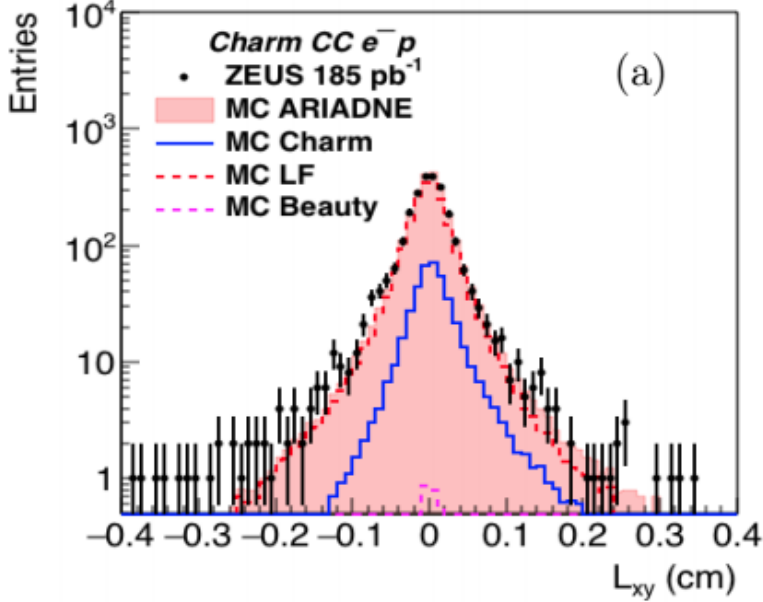


ZEUS

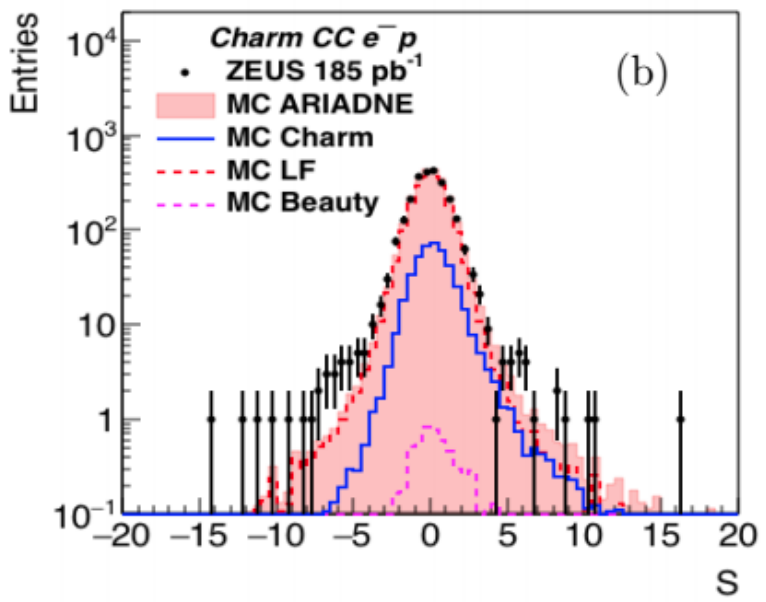


Requested for Paper

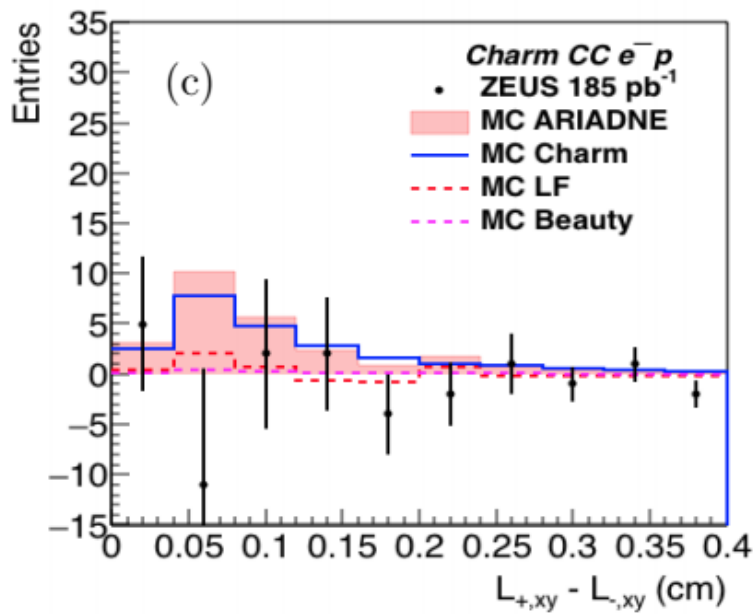
ZEUS



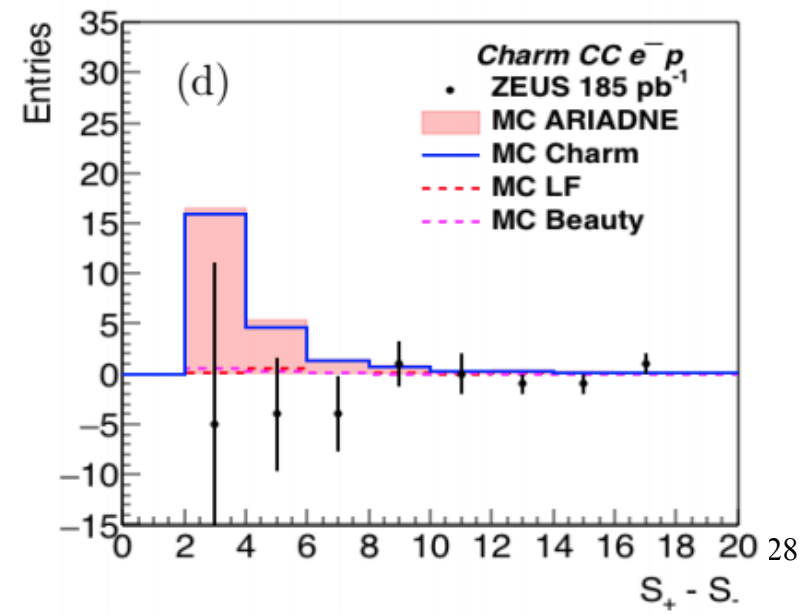
ZEUS



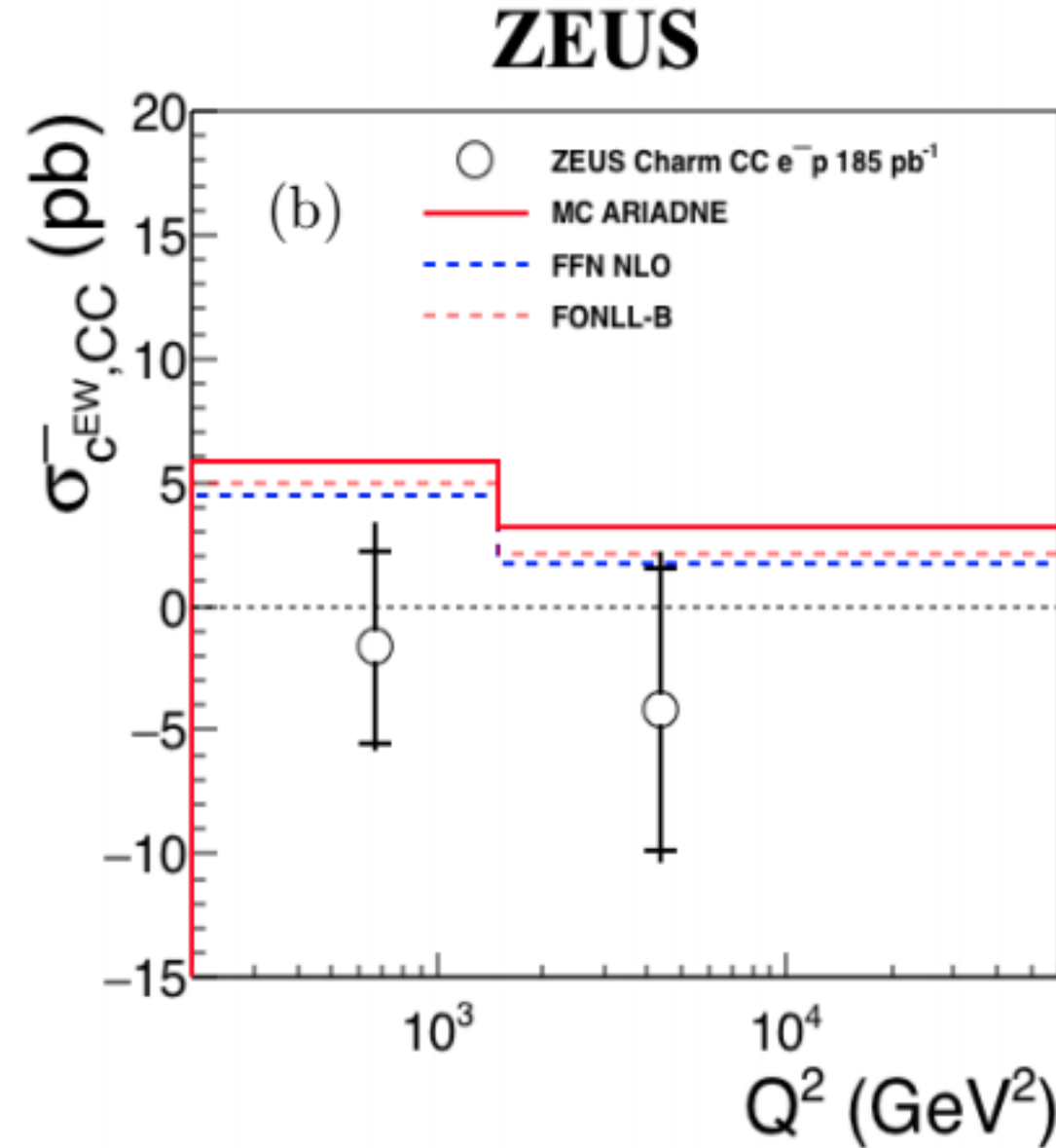
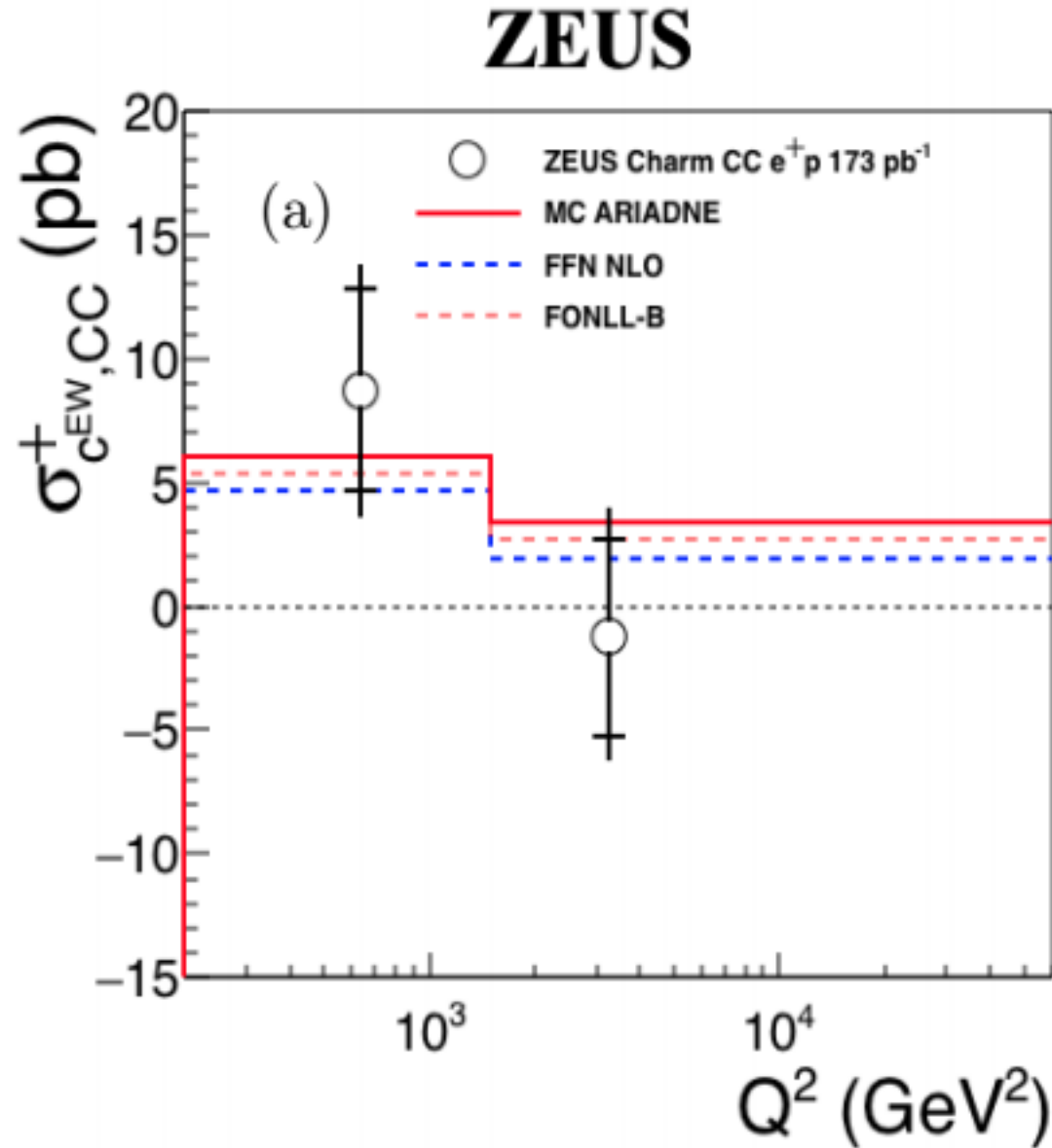
ZEUS



ZEUS



Requested for Paper



Summary

- Measurements on EW Charm production in CCDIS has been performed; separately for e^+p and e^-p .
 - EW charm production has been measured within a kinematic region $200 < Q^2 < 60000 \text{ GeV}^2, y < 0.9, E_T^{jet} > 5 \text{ GeV}$ and $-2.5 < \eta^{jet} < 2.0$
 - Two major contributors are the QPM process $s \rightarrow c$ and BGF process $g \rightarrow c\bar{s}$ sharing about equal contribution.
 - New definition for visible cross sections.
 - Jet & secondary vertex control plots for the paper.
- Further discussion ...
 - Definitions of the kinematic variables. ** first order QED radiative correction & complete one-loop virtual corrections included in HERACLES.
 - Theory predictions to be included (ZMVFNS with HERAPDF2.0, ATLAS-eWZ16-EIG).
 - The correlations between the bins and how to account for them as systematic uncertainty.

Back Up



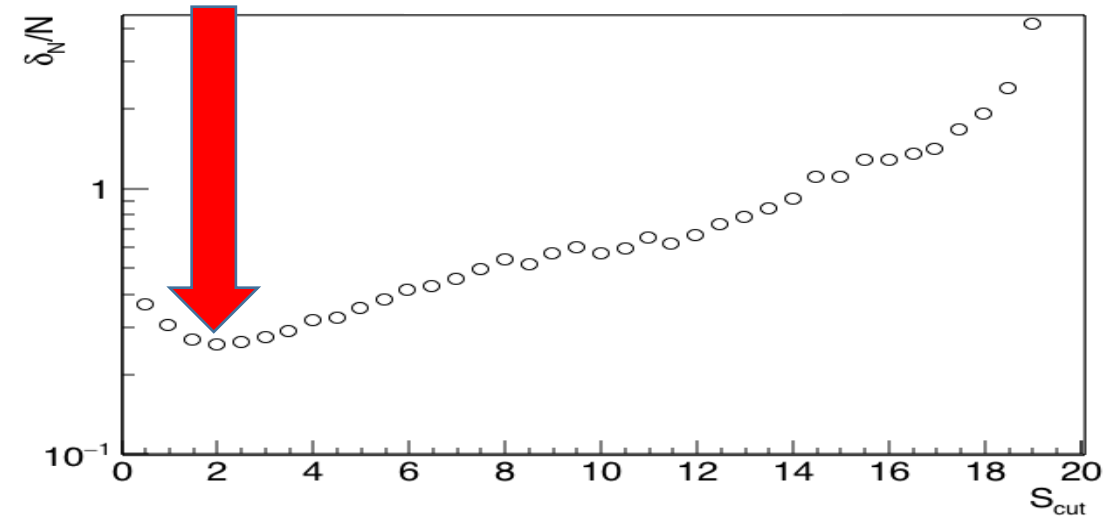
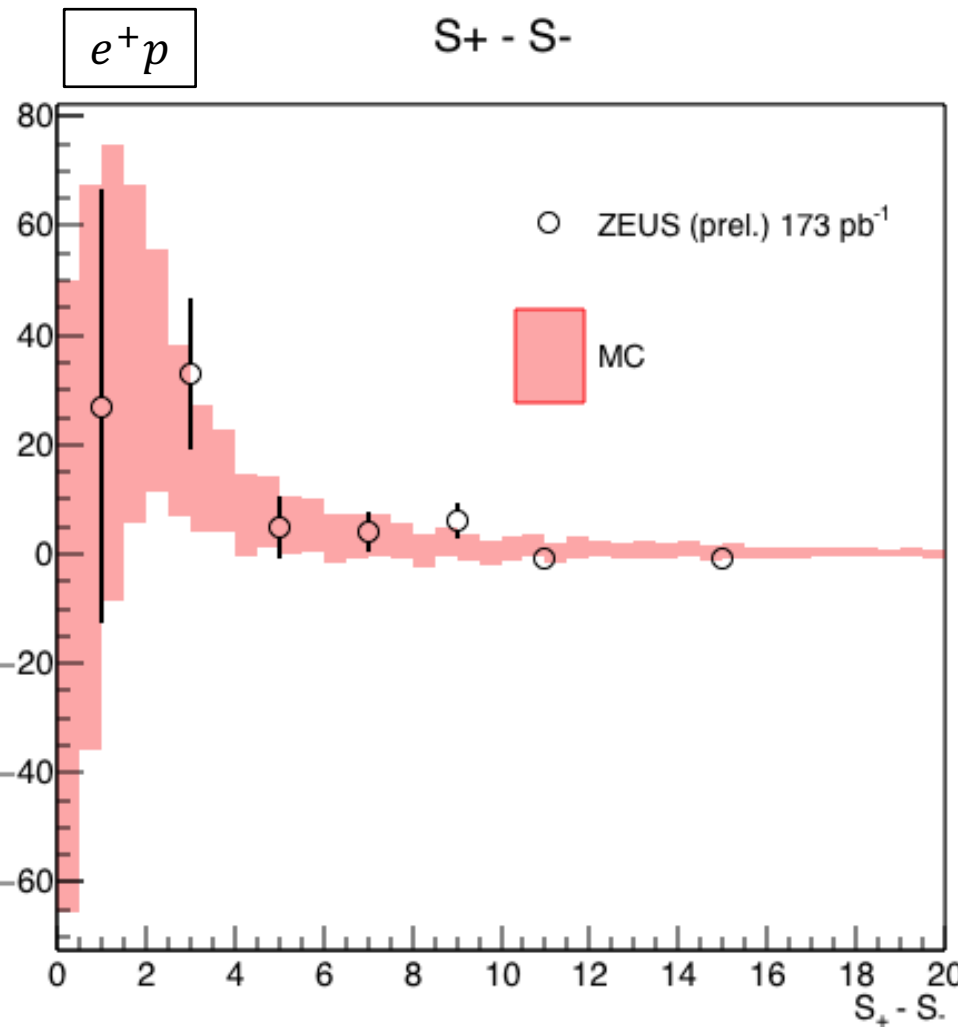
11/19/18

Jae D. Nam

31

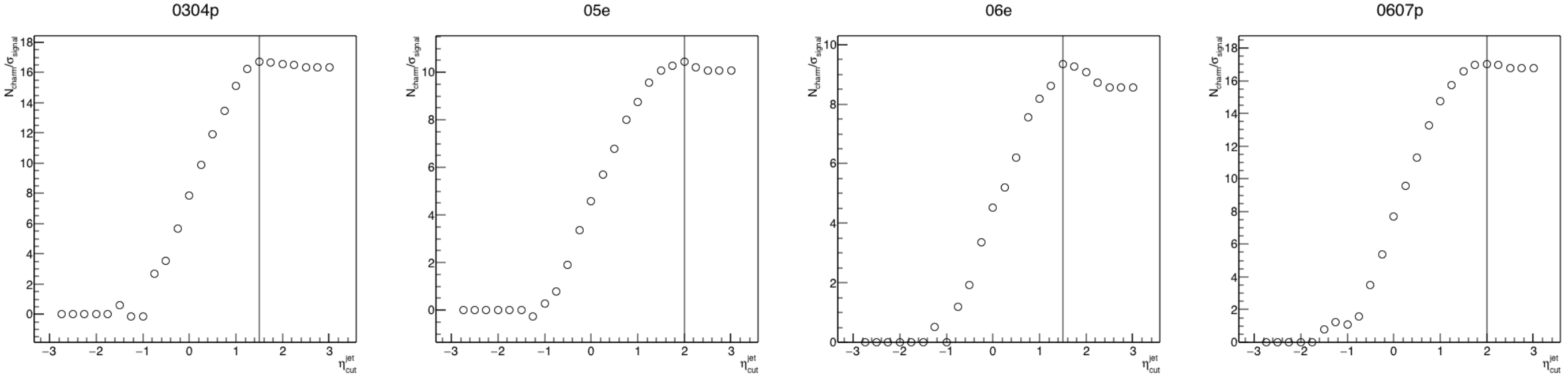


Determination of Significance Threshold



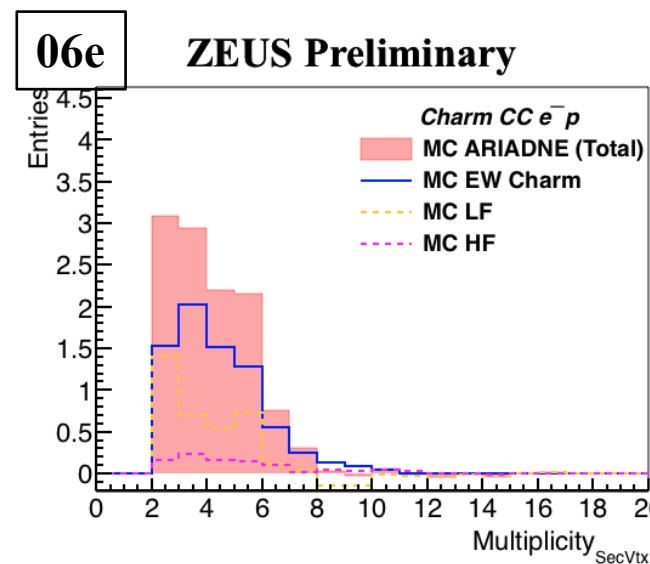
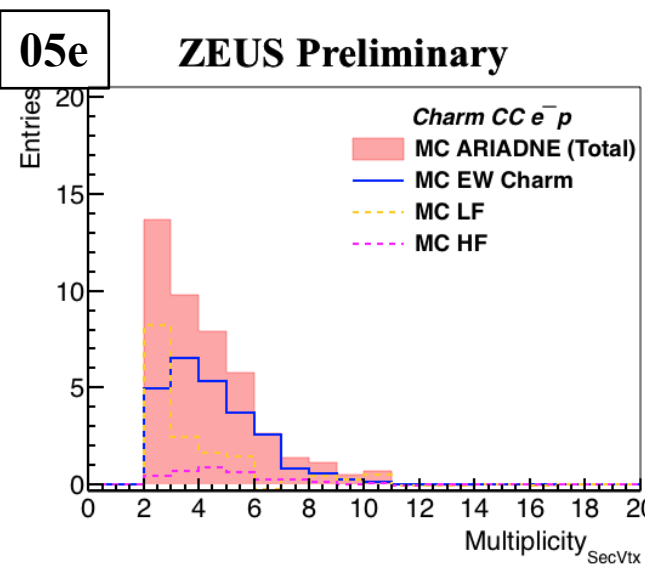
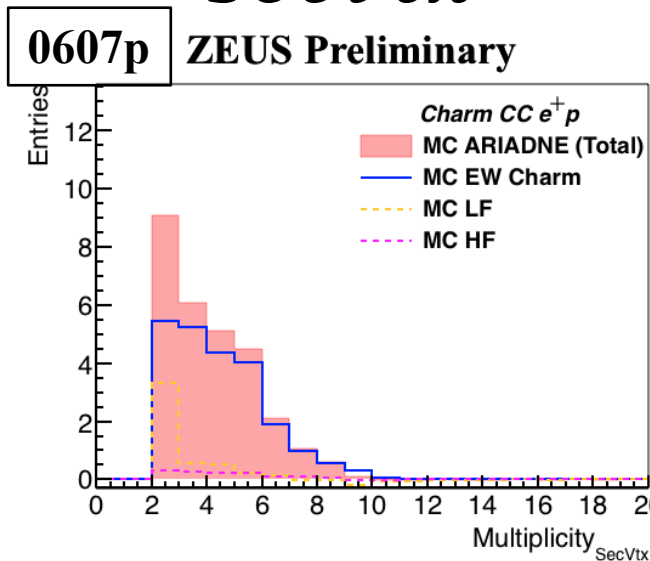
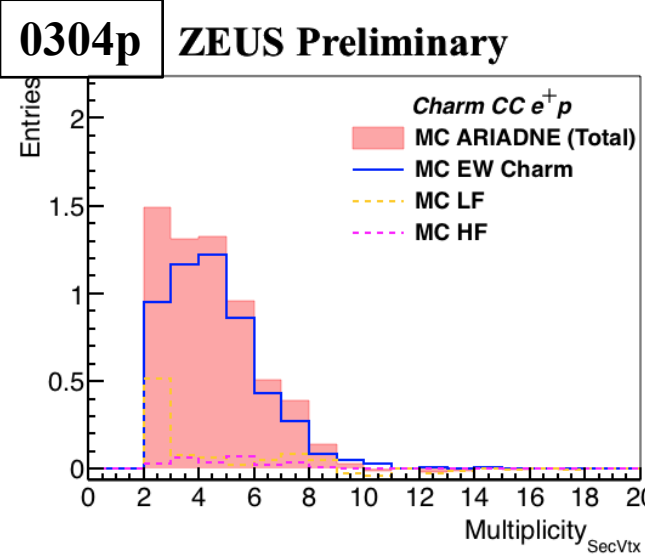
- The high symmetry and large statistics around $S \sim 0$ contributes to a large statistical uncertainty.
- A significance threshold cut was applied to reduce overall statistical uncertainty.
- From MC, the lowest δ/N is achieved if cut were to be applied at $S = 2$.

Determination of η^{jet} upper cut



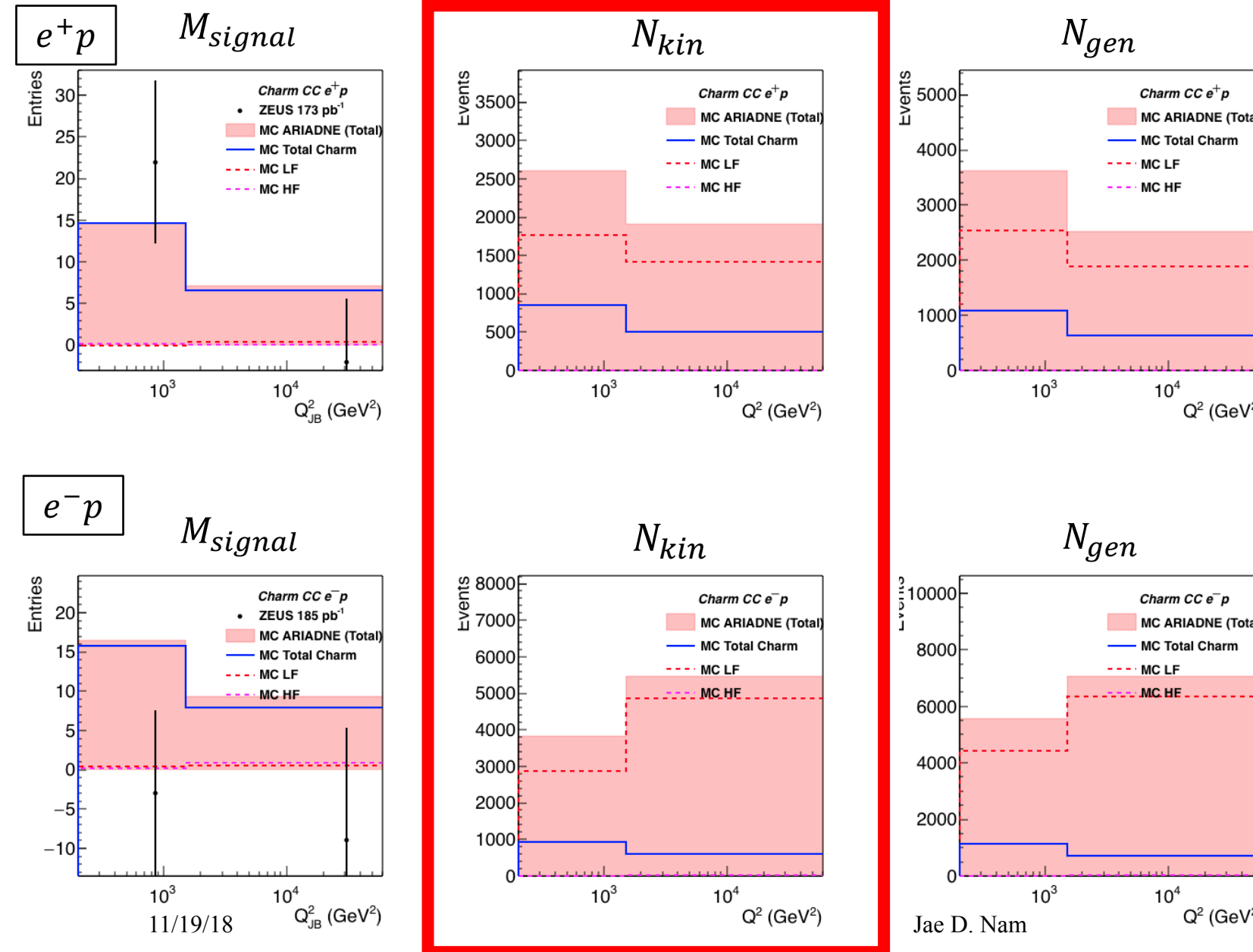
- $\frac{N_{\text{charm}}^{MC,\text{mir}}}{\sigma_{\text{signal}}^{MC,\text{mir}}}$ projected from MC as functions of η_{cut}^{jet} per different run period.
 - Highlighted in red vertical lines are the cut locations that would yield the highest ratio.
- In this presentation, $\eta^{jet} < 1.5$ for 05e (STT coverage), $\eta^{jet} < 2.0$ for else.
 - If not placed on the optimal position, the new η^{jet} cut will not reduce statistical uncertainty significantly.

Determination of N_{secvtx}^{trk} cut



- A high concentration of LF background in low N_{secvtx}^{trk} region is observed across all run periods.
- A LF rejection cut was applied at $N_{secvtx}^{trk} > 2$.

Charm signal & Charm generated (Nov 7)



- Visible total charm cross section:

$$\sigma_{c,vis} = \frac{M^{DATA} - M_{bg}^{MC}}{M_{charm}^{MC}} \frac{N_{kin}^{MC}}{L}$$

- Visible EW charm cross section:

$$\sigma_{c^{EW},vis} = \frac{N_{EW,gen}^{MC}}{N_{gen}^{MC}} \sigma_{c,vis}$$

- Absolute EW charm cross section:

$$\sigma_{c^{EW}} = \frac{N_{gen}^{MC}}{N_{kin}^{MC}} \sigma_{c^{EW},vis}$$

Reconstructed variables

- Good agreement between True and Reconstructed Q^2

$$N_i = \sum_j C_{ij} M_j$$

N_i = true number of entries in bin i
 M_i = reconstructed number of entries in bin i
 C_{ij} = correlation matrix element for bin i,j

Collision	C_{11}	C_{22}
$e^+ p$	0.99	1.01
$e^- p$	0.98	1.02

